Leaf traits and temperature shape the elevational patterns of phyllosphere microbiome

Xing Wang, Zuoqiang Yuan, Arshad Ali, Teng Yang, Fei Lin, Zikun Mao, Ji Ye, Shuai Fang, Zhanqing Hao, Yoann Le Bagousse-Pinguet

Journal of Biogeography

Elevational patterns and drivers of phyllosphere microbial diversity

Journal:	*Journal of Biogeography*
Manuscript ID	JBI-22-0288.R1
Wiley - Manuscript type:	Research Article
Date Submitted by the Author:	20-Oct-2022
Complete List of Authors:	Wang, Xing; CAS Key Laboratory of Forest Ecology and Management Institute of Applied Ecology Chinese Academy of Sciences Shenyang China Yuan, zuoqiang; CAS Key Laboratory of Forest Ecology and Management Institute of Applied Ecology Chinese Academy of Sciences Shenyang China; Northernwest Polytechnical University, School of Ecology and Environment Ali, Arshad; Forest Ecology Research Group College of Life Sciences Hebei University Baoding 071002 Hebei China Yang, Teng; State Key Laboratory of Soil and Sustainable Agriculture Institute of Soil Science Chinese Academy of Sciences East Beijing Road 71 Nanjing 210008 China Lin, fei; CAS Key Laboratory of Forest Ecology and Management Institute of Applied Ecology Chinese Academy of Sciences Shenyang China Mao, Zikun; CAS Key Laboratory of Forest Ecology and Management Institute of Applied Ecology Chinese Academy of Sciences Shenyang China Ye, Ji; CAS Key Laboratory of Forest Ecology and Management Institute of Applied Ecology Chinese Academy of Sciences Shenyang China Fang, Shuai; CAS Key Laboratory of Forest Ecology and Management Institute of Applied Ecology Chinese Academy of Sciences Shenyang China Hao, Zhanqing; School of Ecology and Environment Northernwest Polytechnical University China Wang, xugao; CAS Key Laboratory of Forest Ecology and Management Institute of Applied Ecology Chinese Academy of Sciences Shenyang China; Institute of Applied Ecology Chinese Academy of Sciences, Key Laboratory of Terrestrial Ecosystem Carbon Neutrality Pinguet, Yoann; Aix Marseille Univ CNRS Avignon Université IRD IMBE Technopôle Arbois-Méditerranée Bât Villemin –BP80 Aix-en-Provence cedex 04 France
Key Words:	Biodiversity, Climate, Elevation, Plant functional traits, Plant-microbe associations, Microbial ecology

Elevational patterns and drivers of phyllosphere microbial diversity

Xing Wang[1,2], Zuoqiang Yuan[1,3*], Arshad Ali[4], Teng Yang[5], Fei Lin[1], Zikun Mao[1], Ji Ye[1], Shuai Fang[1], Zhanqing Hao[3], Xugao Wang[1], Yoann Le Bagousse-Pinguet[6]

[1]CAS Key Laboratory of Forest Ecology and Management, Institute of Applied Ecology, Chinese Academy of Sciences, Shenyang, China

[2]University of Chinese Academy of Sciences, Beijing 100049, China

[3]School of Ecology and Environment, Northernwest Polytechnical University, China

[4]Forest Ecology Research Group, College of Life Sciences, Hebei University, Baoding 071002, Hebei, China

[5]State Key Laboratory of Soil and Sustainable Agriculture, Institute of Soil Science, Chinese Academy of Sciences, East Beijing Road 71, Nanjing 210008, China

[6]Aix Marseille Univ, CNRS, Avignon Université, IRD, IMBE, Technopôle Arbois-Méditerranée Bât. Villemin –BP80, Aix-en-Provence cedex 04, France

Author for correspondence: Zuoqiang Yuan (zqyuan@iae.ac.cn)

Abstract:

Aim: Phyllosphere microbial diversity (PMD) is a central biodiversity component for plant health, distribution, and ecosystem functioning. Yet, how climate and leaf functional traits of host plants simultaneously shape elevational patterns of PMD is unclear; but it could improve our ability to predict plant performance and distributions and ecosystem functioning under environmental changes.

Location: Temperate forests of Changbai Mountain Natural Reserve, China

Methods: We investigated changes in the species richness and Shannon's diversity of endo- and epiphytic phyllosphere fungal and bacterial communities, and their covariations, along an 1150 m elevational gradient. We also examined the direct and indirect effects of climate (mean annual temperature; MAT) and thirteen leaf morphological and chemical traits on PMD patterns.

Results: We observed a monotonous decline in PMD with increasing elevation, contrasting with the hump-shaped biodiversity patterns that are commonly reported. Host plant traits – those involved in resource uptake and leaf surface temperature – predominantly shaped the elevational patterns of endophytic PMD, whereas MAT mostly increased the richness and Shannon's diversity of epiphytic organisms. We also observed weak, but significant indirect effects (up to 10%), highlighting that host plant traits are important biotic drivers mediating climate effects on endophytic PMD. Also, no covariation between bacteria and fungi was observed (neither for endophytic nor for epiphytic organisms), supporting neutral associations between bacterial and fungal communities, irrespective of the elevation.

Main conclusions: Our results suggest considering both direct and mediating effects of plant traits to better understand the drivers shaping the richness and Shannon's diversity of endo- and epiphytic phyllosphere microbiomes, and more generally the plant-microbe associations. Our

study also offers a trait-based attempt to disentangle the effects of biotic and abiotic filters in shaping endo- and epiphytic phyllosphere microbial diversity along an elevational gradient.

Keywords: Biodiversity, Climate, Elevation, Plant functional traits, Plant-microbe associations, Microbial ecology.

Introduction

The phyllosphere – the aboveground part of plants – constitutes the largest surface area that microbes inhabit on Earth, and is being estimated to be twice of the global land area (Vorholt, 2012; Zhu et al., 2021). The phyllosphere homes a large variety of phyllosphere microbes, including endophytic and epiphytic fungi and bacteria (Phyllosphere Microbial Diversity; hereafter PMD) (Vorholt, 2012). PMD is a central biodiversity component, largely involved in plant health and performance, influencing ecosystem functioning and supporting crop production (Vacher et al., 2016; Wang et al., 2021). Occurring at the interface between the leaf and the atmosphere, PMD perceives the influences of abiotic (climate) and local biotic conditions (i.e. the host plants). Investigating how PMD simultaneously responds to abiotic and biotic conditions constitutes a great opportunity to better understand how the multiple environmental drivers shape phyllosphere microbial communities, and may offer opportunities to better predict plant performance and distribution, as well as ecosystem functioning under global environmental changes.

Mountain ranges harbor many species endemic to high-elevation habitats, and exhibit multiple but steep environmental changes at relatively small horizontal distances (Bryant et al., 2008; Körner, 2000). For these reasons, elevational diversity gradients received considerable attention (Rahbek et al., 2019). Organismal diversity could follow the early reported decreasing pattern with higher elevation (Von Humboldt & Bonpland, 1805), following the notion that the environment selects for a narrow and similar set of species (The environmental filtering hypothesis) (Le Bagousse-Pinguet et al., 2017; Weiher, Clarke, & Keddy, 1998). However, a hump-shaped pattern of diversity peaking at mid-elevations is likely to occur most commonly (Rahbek, 1995). These diversity patterns have been documented for multiple taxa, such as soil microbes (Bryant et al.,

2008), insects (Machac, Janda, Dunn, & Sanders, 2011; Sanders, 2002), birds (Duclos, DeLuca, & King, 2019), and plants (Grytnes & Beaman, 2006; Le Bagousse-Pinguet et al., 2018). However, we yet lack a clear understanding on how elevational - and underlying abiotic - gradients shape endo- and epiphytic PMD simultaneously. Determining whether PMD follow any particular pattern, and whether they follow the trends observed for other taxa may not only help to better understand the drivers shaping PMD patterns, but also extend, confirm, or refine the existing elevational diversity gradients to unknown taxa.

Elevational diversity patterns have, yet, barely considered fine-scale biotic filters. For instance, the presence of cushion plants, either being competitive or offering micro-refuges, could mediate phylogenetic patterns of plant diversity along elevational gradients (Butterfield et al., 2013; Cavieres et al., 2014; Le Bagousse-Pinguet et al., 2018). Similarly, we could expect that host species act as an important biotic filter shaping, confounding or even altering the overall elevational patterns of PMD. The selection effect of plant host on phyllosphere microbes largely depends on plant attributes (i.e. plant functional traits) (Carvalho & Castillo, 2018; Jia, Yao, Guo, Wang, & Chai, 2020; Leveau, 2019; Vacher et al., 2016). Because plant functional traits relate to how species acquire and conserve resources (Díaz et al., 2007), they represent good proxies of the local biotic environment where phyllosphere microbial communities survive. In such a context, phyllosphere bacterial communities were tightly coupled with leaf dry matter content and leaf area, two plant functional traits involved in resource uptake (Kembel et al., 2014), while fungal communities mostly responded to leaf nitrogen content and specific leaf area (Kembel & Mueller, 2014). However, host plants and their traits may exert greater impacts on the microbe colonization of internal tissues than on that of leaf surfaces, leading to potential distinct responses of epiphytic and endophytic microbes to the environment (Yao, Sun, He, Li, & Guo, 2020; Yao et al., 2019).

For instance, endophytic fungi directly acquire nutrients from inner plant tissues, whereas epiphytic microbes in contact with the external environment mostly depend on the amount of nutrients either exuded from leaves or depositing from the atmosphere (Inácio et al., 2002). Hence, deciphering the relative effects of abiotic and biotic filters simultaneously shaping endo- and epiphytic PMD patterns remains unclear (Agler et al., 2016; Cordier et al., 2012; Wei et al., 2022), and constitutes an important step in our understanding of plant – microbe associations.

Associations (covariations) between bacteria and fungi can arise from a diverse range of interactions, from negative to neutral or even positive. Negative associations could occur as a signature of competition for space and resources (Bahram et al. 2018), while niche partitioning may promote positive covariations as a result of fitness differences among organisms (Bruno, Stachowicz, & Bertness, 2003). For instance, fungal organic matter degradation has been shown to benefit bacteria (Boer, Folman, Summerbell, & Boddy, 2005). Yet, whether and how abiotic and biotic filters shape PMD associations remains poorly investigated (Agler et al., 2016; Cordier et al., 2012; Wei et al., 2022), even though describing how complex interactions among microbial communities could largely matter for the health of plants.

Here, we investigated changes in the species richness and Shannon's diversity index of endo- and epi-phytic phyllosphere fungi and bacteria, and their covariations, along a steep 1150 m elevational gradient. We addressed the following questions and associated hypotheses: Q1) Does PMD exhibit particular elevational patterns? H1) We hypothesized that the diversity of phyllosphere microbes follows a mid-elevational gradient pattern, corresponding to the most common pattern observed across taxa. Q2) Do phyllosphere endo- and epiphytic microbes respond similarly to abiotic and biotic filters? H2) We hypothesized that endophytic microbes are more sensitive to the biotic filter (i.e., host plant traits), whereas epiphytic microbes mostly respond to

climate. Q3) How do abiotic and biotic filters shape PMD covariations? H3) We hypothesized prominent negative relationships as a signature of competition for space and resources, and the elevational gradient to modulate these associations.

Material and Methods

Study site and climate data

The study site is located in the Changbai Mountain Natural Reserve (127° 42′ to 128° 17′ E, 41° 43′ to 42° 26′ N) in the Jilin province of northeastern China (Fig. 1a), which is one of the largest protected temperate forests around the world (Stone, 2006; Wang et al., 2013). The reserve covers approximately 200, 000 ha, with an elevation range between 740 and 2691 m a.s.l. The area is strongly influenced by the monsoon and experiences a temperate continental mountain climate with long, cold winters and warm summers. The predominant soil type of the studied area is Alfisol according to the US soil taxonomy (Mao et al., 2019; Yang, 1985; Yuan et al., 2013).

The elevational gradient considered in this study ranges from the mountain foot (500 m a.s.l) to the summit (the volcanic crater lake) (2744 m a.s.l.) (Fig. 1b), where the mean annual temperature declines from 3.5 to -7.4 °C, but the mean annual precipitation (MAP) increases from 632 to 1154 mm. The elevational gradient encompasses four distinct vegetation zones: the broad-leaved Korean pine (*Pinus koraiensis*) mixed forest (500 m–1100 m), the spruce-fir (*Picea jezoensis* and *Abies nephrolepis*) forest (1100–1800 m), the subalpine birch (*Betula ermanii*) forest (1800–2000 m) and an alpine tundra zone (above 2100 m). Along with a horizontal distance of about 40 km, these four forest types represent a condensed picture of the array of vegetation landscapes from the temperate zone to the polar region (Shao, Schall, & Weishampel, 1994; Yang, 1985). Data of mean annual temperature and precipitation were retrieved from (Shen et al., 2014;

Shen et al., 2013)

Leaf sampling

Leaf samples were collected in August 2020 at 800, 1000, 1200, 1400 1600, 1800 and 1950 m, i.e. at all representative forest zones along the studied elevational gradient (Table S1). At each elevation, we established five 50×50m plots that had an interval of 50 m and sampled 5 samples of each tree species from each elevation (one sample per plot) (Fig1 c). Because the number of dominant tree species differed among elevations (there are 30, 20, 5,10, 20, 10 and 5 samples from the low to high elevation), the total number of samples was not same among elevations (Fig. 1b). In each plot, leaves without signs of disease or feeding damage were collected on one adult tree of each of the dominant species (Table S2). The specialized worker climbed upward the canopy of each tree by foot hook and took three branches from four directions using sterilized scissors. About 80 gram of healthy leaves were taken using sterile gloves and then subdivided into two samples. One sample was stored at 4 ℃ to determine the leaf morphological and chemical properties, while the other sample was stored at –80 ℃ before DNA extraction. A total of 100 leaf samples were sampled from ten tree species (n=100, some species are distributed at multiple elevations).

Leaf functional traits

We measured 13 common leaf morphological and chemical traits related to life history and nutrient and water-use efficiencies (Table S3 & Fig. S1), following standard protocols (Pérez-Harguindeguy et al., 2013). Leaf morphological traits, such as specific leaf area (SLA), reflect light interception ability and trade-offs between the longevity of the plant tissues and construction cost, whereas leaf chemical traits such as leaf carbon (LCC) and leaf nitrogen content (LNC) reflect

photosynthetic and growth ability (Chave et al., 2009). Leaf area (LA) was calculated using a portable scanner (Canon LiDE 110, Tokyo, Japan) and Image-Pro Plus 6.0 software (Media Cybernetics, USA). The mass of dried leaf samples (LDMC) with an accuracy of 0.1 mg was estimated after oven-drying at 65 °C for 48 hours at a constant mass. SLA was calculated as the ratio of projected leaf area to leaf dry mass. A RETSCH MM400 (RETSCH, GmbH, Haan, Germany) was then used to ground the oven-dried leaf samples into a fine powder. Leaf carbon and nitrogen contents were measured using an elemental analyzer (Vario EL III, Elementar, Hanau, Germany. Leaf stable carbon (LCC_{13}) and nitrogen isotope composition (LNC_{15}) was analyzed using the isotopic Cavity-Ring Down Spectrometer with the Combustion Module (CMCRDS system, Picarro, CA, USA). We also measured the following chemical elements: leaf phosphorus content (LPC), leaf potassium content (LKC), leaf copper content (LCuC), leaf calcium content (LCaC) and leaf zinc content (LZnC) using an ICP Optima 8000 (Perkin-Elmer, Waltham, MA, USA).

We used the nail-polish imprint method (Zhao, Chen, Brodribb, & Cao, 2016) to estimate leaf stomatal character. Six leaves were randomly selected from each sample, and the nail polish was applied to the center of the abaxial leaf surface. After the nail polish is dried, the polish was then stripped using sellotape and mounted onto a glass slide. Microphotographs were photographed using a Classica SK200 Digital light microscope (Motic China Group Co., Ltd, China). 3-5 visual fields were randomly selected for each sample in a 40-fold objective lens and a 10-fold eye lens. Leaf stomatal area (LSA) was calculated as the mean value of the product of the length of the long axis and the length of the short axis of the five stomata selected in the random field using Image-Pro Plus 6.0 software (Media Cybernetics, USA).

Leaf DNA extraction and sequencing

Phyllosphere epiphytic microbes were washed from leaf surfaces according to the standard protocols (Yao et al., 2020; Yao et al., 2019). Five g of leaf samples were placed in sterile tubes and 10 ml of sterile cooled TE buffer (10 mM Tris–HCl, 1 mM EDTA, pH 7.5) was added to each gram of samples. Samples were then washed by ultrasonic for 1 min and whirled for 10 s, and repeated twice. The liquids obtained after two cleanings were mixed and passed through a 0.2 μm sterile filter membrane (SUPOR, Pall Corporation). The filtered membrane was transferred to the freezer at -80 °C for analysis (Herrmann, Geesink, Richter, & Küsel, 2021). Samples of endophyte microbes were isolated from the same plant leaves used for isolating epiphytes. The leaves were submerged for 1 min with 75% ethanol, 3.25% sodium hypochlorite for 3 min, 75% ethanol for 30 s, and eventually rinsed 3 times with sterile distilled water. Each sample was ground in liquid nitrogen using a mortar and pestle, and then only 5 g of leaf powder was retained for DNA extraction (Bodenhausen, Horton, & Bergelson, 2013).

Total genomic DNA was extracted by the FastDNA® SPIN Kit (Qbiogene, Irvine, CA) according to the manufacturer's instructions. The DNA extract was checked on 1% agarose gel, and DNA concentration and purity were determined with NanoDrop 2000 UV-vis spectrophotometer (Thermo Scientific, Wilmington, USA). For bacteria, we targeted V5-V7 region of the 16S rRNA gene, using 799F (AACMGGATTAGATACCCKG) and 1193R (ACGTCATCCCCACCTTCC). Two step PCR were used to amplify phyllosphere endophytic bacteria. This method and the primer we choose can guarantee good coverage of endophytic bacteria taxa (Bulgarelli et al., 2015; Bulgarelli et al., 2012; Giangacomo, Mohseni, Kovar, & Wallace, 2021; Lundberg et al., 2012). The PCR amplification was performed as follows: initial denaturation step at 95°C for 3 min, the targeted region was amplified by 27 cycles of 95°C for 30

s, 55°C for 30 s and 72°C for 45 s, followed by a final elongation step of 10 min at 72°C with the 799F and 1392R (ACGGGCGGTGTGTRC) primers. With sterile deionized water, the initial PCR product was diluted by a factor of 50. 1.0 μ L of the diluted solution was used. The second-step primers were 799F-1193R and identical conditions to the first step except for the number of PCR cycles that was lowered to 13. For fungi, we targeted the ITS1 region of the rRNA operon, using the ITS1F (CTTGGTCATTTAGAGGAAGTAA) and ITS2R (GCTGCGTTCTTCATCGATGC). The PCR amplification was performed as follows: initial denaturation at 95 ℃ for 3 min, followed by 35 cycles of denaturing at 95 ℃ for 30 s, annealing at 55 ℃ for 30 s and extension at 72 ℃ for 45 s, and single extension at 72 ℃ for 10 min, and end at 10 ℃. PCR amplification was performed for both the 16 S rRNA gene and the ITS1 region with 20 μl reaction system, containing 5 × TransStart FastPfu buffer 4 μL, 2.5 mM dNTPs 2 μL, forward primer (5 μM) 0.8 μL, reverse primer (5 μM) 0.8 μL, TransStart FastPfu DNA Polymerase 0.4 μL, template DNA 10 ng, and finally ddH2O up to 20 μL. PCR reactions were performed in triplicate. The PCR product was extracted from 2% agarose gel and purified using the AxyPrep DNA Gel Extraction Kit (Axygen Biosciences, Union City, CA, USA) according to the manufacturer's instructions and quantified using Quantus™ Fluorometer (Promega, USA). The raw data were sequenced on an Illumina NovaSeq PE250 platform (Illumina, San Diego, USA) by Majorbio Bio-Pharm Technology Co. Ltd. (Shanghai, China).

Bioinformatic analyses

The raw gene sequencing reads were filtered using QIIME (version 1.7) (http://qiime.org/tutorials/tutorial.html). Low-quality sequences (length<200 bp), ambiguous bases>0, average base quality score<25) were removed. Samples were distinguished according to the

barcode and primers, and the sequence direction was adjusted. The amplicon length ranges for 16S are 593bp (the first PCR) and 394bp (the second PCR), and the amplicon length ranges for ITS is 300bp (Yang et al., 2019). Only overlapping sequences longer than 10 bp were assembled according to their overlapped sequence. The maximum mismatch ratio of the overlap region is 0.2. Reads that could not be assembled were discarded; Samples were distinguished according to the barcode and primers, and the sequence direction was adjusted, exact barcode matching, 2 nucleotide mismatch in primer matching.The sequences were then clustered into operational taxonomic units (OTUs) with 97% similarity cutoff using UPARSE version 7.1 (Edgar, 2013), and chimeric sequences were identified and removed. The taxonomy of each OTU presentative sequence of bacteria and fungi was assigned by RDP Classifier version 2.2 (Wang, Garrity, Tiedje, & Cole, 2007) against the Silva v138 with a confidence cut-off (*P*) value of 0.80 and UNITE 8.0 with a confidence cut-off (*P*) value of 0.70, respectively. The OTUs that were not classified into bacteria or fungi were removed. In total, we obtained 12,218,626 and 11,031,668 high-quality sequences for fungi and bacteria separately. After rarefying all samples to an equal sequencing depth (21898 reads per sample), the fungal and bacterial communities included 3110 and 5231 OTUs, respectively. The proportion of Chloroplasts (4/3173) and Mitochondria (30/3173) in the total number of OTUs was acceptable, and did not affect our analysis.

Statistical analyses

To evaluate the elevational patterns of PMD, we conducted linear mixed models with the Shannon index (H) (average value of each plot) and negative binomial generalized linear models with the richness (S) (average value of each plot) of all (i.e., epiphytic + endophytic), endo- and epiphytic bacteria and fungi as response variables, whereas elevation and elevation^2 (i.e. to test for potential

humped-shaped relationships) as predictors, and the plot as a random factor. We used negative binomial generalized linear models to account for the richness of microbes (e.g. the number of OTUs) in count data (Shrestha, Su, Xu, & Wang, 2018). Models were sorted and compared according to the Akaike Information Criterion (AIC) and the likelihood ratio test.

We performed a heatmap plot to illstrate the relationships between plant functional traits and specific microbial taxa by "*corrplot*" package (Wei et al., 2017). We further performed a principal component analysis (PCA) on the nine least correlated leaf traits (over the 13 traits originally considered; Fig. S1). This approach approximates the functional space that species occupy and defines their position in multi-dimensional trait space (Devictor et al., 2010). The first axis of PCA (FT_{PC1}) explained 46.9% of the total variation in trait variables. This axis mainly correlated with high leaf area and SLA (Table S4), thus discriminating leaf traits associated with the leaf economic spectrum (LES; Wright *et al*., 2004). The second axis (FT_{PC2}) explained 28.7% of the total variation in trait variables, and mainly correlated with micronutrients such as leaf copper and zinc contents. The two PCA axes were used in subsequent analyses because they are independent variables at the species level and reflect important leading dimensions of the species niche (Gross et al., 2013).

To evaluate the simultaneous effects of abiotic (climate) and biotic (leaf traits) conditions on endo- and epiphytic PMD, we performed linear mixed models with H and with S of all, endo- and epiphytic bacteria and fungi as response variables. We included MAT and MAT^2 as climate predictors (MAP was considered, but removed due to its high correlation with MAT and less importance in the models; Fig. S1), FT_{PC1} and FT_{PC2} as biotic predictors, and site included as a random factor. Response variables were log-transformed when necessary to normalize data distribution prior to analyses to meet the assumptions of the test used. All predictors were

standardized using the Z-score to interpret parameter estimates on a comparable scale. Models were ranked according to the lowest AICc, and retained within ΔAIC <2. Standardized regression coefficients (β) were obtained using a model averaging approach. Since all predictors and response variables were standardized, an analogue of the variance decomposition analysis was applied to obtain the relative importance of each predictor based on the marginal R^2, which can be simply calculated as the ratio between its standardized regression coefficient and the sum of all coefficients, and expressed in % (Le Bagousse-Pinguet et al., 2019; Yuan et al., 2021).

Finally, piecewise structural equation models (pSEMs) were performed to investigate direct and indirect pathways of the abiotic and biotic influences on PMD and their associations (the conceptual model is provided in Fig. S4). Each predictor's indirect impact was estimated by combining the standardized direct effect of a predictor on a mediator with the direct influence of a mediator on the response variable. The total effect of predictors is calculated as the sum of direct and indirect effects (Yuan et al., 2020). Based on a priori theoretical knowledge, we hypothesized that functional traits and climate factors simultaneously would have a direct impact on PMD (e.g. S of bacteria and fungi), and climate factors also would have an indirect impact on PMD via altering functional traits. We also considered potential relationships between bacteria and fungi to evaluate the strength and direction of their associations using linear mixed models in pSEM analyses. Site was used as a random factor. Model parameters and fit were assessed using Fisher's C statistic. Models with adequate fit to the data had a Fisher's C statistic with $p > 0.05$ (Shipley, 2009). The pSEM analyses were performed using "piecewiseSEM" package (Lefcheck, 2016). The pSEMs were tested for S and H of phyllosphere epiphytic, endophytic and all microbial groups (epiphytic + endophytic).

All statistical analyses were performed in the R 4.1.0 software (http://www.r-project.org/).

The negative binomial generalized linear models were conducted using the *MASS* package. The linear mixed models were conducted using the *lme4* package, and model selection was performed using the "dredge" function in the *MuMIn* package (Bartoń, 2020).

Results

We found that endo- and epiphytic bacteria were mainly composed of Proteobacteria and Actinomycetes, while phyllosphere fungi were mainly represented by Ascomycetes and Basidiomycetes (Appendix Fig. S2 & S3). Proteobacteria (the most dominant bacterial group) were evenly distributed among the studied tree species, while the dominat groups of fungi (Ascomycetes) were mainly associated to *Larix_gmelinii* and *Betula_ermanii*. The phyllosphere microbes mostly occurred at low (800m) and mid-elevation (1600m).

For all studied response variables, the best—fitted models included elevation only as a predictor (Fig.2; Appendix Tables S5 & S6). We observed a linear decrease pattern in richness (S) and Shannon index (H) for both bacterial and fungal communities along the studied elevational gradient. We observed a steeper decline in epiphytic bacterial diversity ($Baceria_{Epip}$) than in endophytic bacteria ($Baceria_{Endo}$) (ANOVA test' $P < 0.001$, Fig.1), whereas endophytic fungi ($Fungi_{Endo}$) decreased more dramatically along the elevational gradient than epiphytic fungi ($Fungi_{Endo}$) (ANOVA test' $P < 0.001$).

The climate (MAT) and the multiple leaf traits accounted for a fair amount of explained variance across the richness (S) of phyllosphere microbes (from 50 to 66%), and notably for epiphytic fungi (Fig.3f). Mean annual temperature (MAT) explained on average 27% of variations (19%–37%) in S of phyllosphere microbes. The climate (MAT) and the multiple leaf traits explained a slightly higher amount of variance (from 56% to 69%) for the Shannon index (H), and

notably for the epiphytic fungi (Fig.S5f). Mean annual temperature (MAT) explained up to 30% (22%–38%) of variations in H of phyllosphere microbes. MAT was significantly associated with higher S and H of microbial communities, indicating that higher temperature linearly increased both the richness and Shannon's diversity of microbes (MAT^2: $p > 0.05$). The first axis of PCA on functional traits (FT_{PC1}) – related to the LES - explained up to 26% (13%–37%) and 28% (15%–41%) for S and H, respectively. Higher leaf area and SLA (and lower LDMC) thus increased the S and H of both bacterial and fungal communities. In contrast, the second axis of PCA on functional traits (FT_{PC2}) accounted for only 1.2% (1.1%–1.4%) of variations in PMD (Fig.3 &Fig.5).

The final pSEMs indicated that all PMD metrics were not only associated with direct changes in MAT and leaf traits but also through indirect pathways (Fig. 4; Appendix Table S7 & S8). Indirect effects represented up to 12% of variations in PMD. Phyllosphere bacterial S and H were thus directly influenced by MAT (β=0.305–0.535) and FT_{PC1} (β=0.258–0.419), and indirectly affected by trait-mediated effects of MAT (β= 0.058–0.094). The average total impact (all, endophytic and epiphytic) of MAT on phyllosphere bacterial S and H was 0.485 and 0.504, respectively. Phyllosphere fungal S and H were directly influenced by MAT (β=0.498–0.603) and FT_{PC1} (β=0.333–0.508), but indirectly affected by trait-mediated effects of MAT (β= 0.074–0.114). The average total impact (all, endophytic and epiphytic) of MAT on phyllosphere fungal S and H index were 0.515 and 0.544, respectively. Also, the effects of MAT and FT_{PC1} on phyllosphere fungi (0.388-0.603 and 0.333-0.508) were greater than those on phyllosphere bacteria (0.305-0.535 and 0.258-0.424). In sum, the effects of MAT on phyllosphere epiphytic microbes (0.524-0.603) were greater than those on phyllosphere endophytic microbes (0.305-0.571). The effects of FT_{PC1} on phyllosphere endophytic microbes (0.417-0.508) were greater than those on phyllosphere

epiphytic microbes (0.258-0.359). Finally, we did not observe any correlations between bacteria and fungi, neither for endophytic nor epiphytic microbes (P>0.05). In addition, there was no strong change in the pSEMs results across S and H of phyllosphere epiphytic, endophytic and all microbial groups (Figs. 4, S6, S7 and S8).

Discussion

Here, we investigated the elevational patterns of endo- and epiphytic phyllosphere fungal and bacterial communities, and whether underlying climate (MAT) and biotic drivers (the leaf traits of host plants) could explain the observed patterns. We observed a linear decrease in the richness and Shannon's diversity of fungal and bacterial communities along the studied elevational gradient, but contrary to expectation, no covariations between microbial communities were observed. The climate features and leaf plant functional traits shaped the observed monotonous decline of microbial biodiversity, with a higher sensitivity of endophytic microbes to the biotic filter (host plant traits) and epiphytic microbes to climate.

We observed a monotonous decline of phyllosphere microbial diversity with increasing elevation, contrasting with the hump-shaped biodiversity pattern commonly reported across taxa (Rahbek, 1995), and notably for soil microbes (Geml et al., 2022; Kotilinek et al., 2017; Rehakova, Chlumska, & Dolezal, 2011). While restricting our study to areas above 700 m.a.s.l. (i.e. the areas that are the least impacted by human disturbance) may have limited our ability to detect humped-shaped patterns, our observed PMD patterns concurred with that of tropical plant species richness decreasing with elevation (Von Humboldt & Bonpland, 1805); and hence, with the view that the environmental filtering hypothesis (Le Bagousse-Pinguet et al., 2017; Weiher et al., 1998). Our result also matched with the clustering patterns observed for phylogenetic diversity with elevation

for soil microbes (Bryant et al., 2008), insects (Machac et al., 2011; Smith, Hallwachs, & Janzen, 2014), birds (Graham, Parra, Rahbek, & McGuire, 2009), and somehow for plants (Bryant et al., 2008; Zhang, Xiao, & Li, 2015). However, we also observed that the monotonous decline of PMD patterns along the elevational gradient was significantly steeper for epiphytic than endophytic bacteria; but the inverse was observed for fungal communities. These results highlight the complex responses of phyllosphere biological groups to environmental gradients, and the importance to discriminate endo- *vs*. epiphytic microbial communities if we aim at better understanding and predicting microbial changes in response to ongoing environmental changes. Altogether, our study extends our understanding of how elevation shapes the diversity of phyllosphere bacteria and fungi, and brings new evidence that hump-shaped biodiversity patterns may not be as prevalent as previously thought along elevational gradients (Guo et al., 2013; Wang et al., 2017).

Our results reveal that temperature (and the highly collinear effect of the mean annual precipitation (MAP; Appendix Fig. S1)) was a key driver of PMD along the studied gradient, but it predominantly shaped the elevational patterns of epiphytic organisms. While MAT has been recognized as one of the main abiotic drivers of soil microbes along elevational gradients (Nottingham et al., 2018), here we showed that the climate impacts depend on how microbes are exposed to external conditions (Gomes, Pereira, Benhadi-Marín, Lino-Neto, & Baptista, 2018; Vacher, Cordier, & Vallance, 2016). The observed positive temperature-diversity relationship could be explained by the metabolic theory of ecology, i.e., temperature could accelerate the metabolic rates and biochemical processes of organisms (Brown, Gillooly, Allen, Savage, & West, 2004; Gillooly, Brown, West, Savage, & Charnov, 2001). In addition, we observed that MAT has a slightly higher impact on the phyllosphere fungal than on bacterial diversity, concurring with the view that fungi are more sensitive to temperature changes than bacteria (Vacher et al., 2016).

Altogether, our study warns for the potential changes that phyllosphere microbes could experience, and the potential for this central biodiversity component to further alter plant health, diversity and ecosystem functioning under global environmental changes such as warming.

We found a significant effect of leaf functional traits on elevational patterns of PMD. Our result points toward the importance of the functional attributes of host plants for PMD, while we even did not consider plant phylogeny, a biotic driver that encompasses unmeasured biological traits (Flynn, Mirotchnick, Jain, Palmer, & Naeem, 2011)and is relevant for phyllosphere diversity (Leff et al., 2018; Martínez-García, Richardson, Tylianakis, Peltzer, & Dickie, 2015; Yang et al., 2019). Interestingly, we showed that leaf traits were mostly involved in shaping elevational patterns of endophytic PMD, likely because they predominantly depend on the inner plant tissues (Mina, Pereira, Lino-Neto, & Baptista, 2020; Yao et al., 2019). We further observed weak, but significant indirect effects (up to 10%), highlighting that host plant traits are important biotic drivers mediating climate effects on PMD. These indirect effects were 2-fold stronger for endophytic than epiphytic communities, reinforcing the primary role of host plant traits in shaping inner microbial communities. We acknowledge that our study did not consider interactive effects between MAT and the biotic attributes of host plants, and it may have potentially underestimated the strength of climate effects mediated by the local biotic filters. Our data also showed that the effects of host plant traits were slightly stronger on phyllosphere fungal diversity than on bacterial diversity. This result may arise from the higher transport material capacity of fungal mycelium than that of bacteria (Boer et al., 2005; Jennings, 1987). While studies on mountain diversity patterns yet barely considered fine-scale biotic filters, our results clearly highlight the need to consider their direct and mediating effects to better understand plant–microbe associations and the drivers shaping elevational diversity gradients.

The first axis of the PCA was positively related to leaf traits such as leaf area and SLA (and negatively to LDMC; see Appendix Table S4). These leaf traits all belong to the Leaf Economic Spectrum (Wright et al., 2004), one of the major axes of the global spectrum of plant forms and functions (Diaz et al., 2016). They also represent influential plant functional attributes for phyllosphere bacterial (LDMC and LA) and fungal (SLA) diversities (Kembel & Mueller, 2014). Two main reasons could explain the importance of these functional attributes of host plants for phyllosphere microbial diversity. First, they discriminate fast-growing acquisitive strategies and resource uptake in plants (Kembel & Mueller, 2014), and thus relate to the plant's nutritional value (Leveau, 2019; Liu, Brettell, & Singh, 2020 ; Vorholt, 2012). Second, traits such as LDMC have been recently shown to relate to the leaf surface temperature (Liancourt, Song, Macek, Santrucek, & Dolezal, 2020; Michaletz et al., 2015; Yang et al., 2021), a biophysical process involved in plant species distribution along elevational gradients (Liancourt et al., 2020). As such, we may expect that LDMC could also determine the bioclimate that PMD experience, and likely their distributions along environmental gradients. While species-level trait measurements offer insights into PMD patterns, we further advocate for incorporating intraspecific trait variation, a central component influencing plant species interactions (Kraft, Crutsinger, Forrestel, & Emery, 2014; Le Bagousse-Pinguet et al., 2015), and community assembly and dynamics (Bolnick et al., 2011; Violle et al., 2012). Adopting an individual perspective of trait variation may further help to understand PMD patterns, as well as to refine our predictions for community assembly, functional ecology and plant–microbe associations.

Finally, we did not observe any covariation between bacteria and fungi, neither for endophytic nor for epiphytic organisms, irrespective of the diversity metric considered (richness or Shannon's diversity). Our result supports neutral associations between bacterial and fungal communities,

while we expected negative associations to occur as a signature of competition for space and resources (Bahram et al., 2018). Two reasons may explain these results. On the one hand, the absence of a relationship may highlight that stochastic assembly processes dominate as often observed in other hyperdiverse systems such as the tropical forest biome (Harms, Condit, Hubbell, & Foster, 2001). Neutral associations have been, for instance, observed in topsoil microbiomes, particularly in agricultural systems (Jiao et al., 2021). On the other hand, neutral associations could reflect the outcome of antagonistic deterministic processes fluctuating over time to shape microbial communities (Götzenberger et al., 2012; Wang et al., 2016).

Conclusions

Our results offer the first step in understanding PMD associations and call for further investigation to identify the putative underlying processing involved in shaping complex interactions among microbial communities. We found a monotonous decline of phyllosphere microbial diversity with increasing elevation, which contrasts with the commonly reported hump-shaped biodiversity pattern along elevational gradients. Our work also demonstrated that host plant functional traits – those involved in resource uptake and leaf surface temperature – predominantly shape endophytic PMD patterns through both direct and indirect effects, while climate mostly impacted epiphytic microbial communities. Our study provides a first hierarchical framework based on the simple effect of traits to quantify the effects of biotic filters in shaping PMD patterns along ecological gradients, and to disentangle their effects from those of the abiotic environment.

Conflict of Interest Statement

We ensure that none of the authors declared a conflict of interest.

Author contributions

ZY, XW and YLB-P conceived the idea; XW, ZY, FL, ZM, JY, SF, ZH and XW performed the research and collected the data; XW, AA, ZY and YLB-P analysed the data; XW and YLB-P wrote the first draft of the manuscript, and all of the authors contributed substantially to the revisions.

Data Availability

Microbe data are available from the NCBI Sequence Read ArchivAeArchive (SRA) database (Accession Number: PRJNA824213), other data that support the findings of this study are available from the corresponding author upon reasonable request.

Acknowledgements

This work was supported by the Strategic Priority Research Program of the Chinese Academy of Sciences (XDA 23080301 & XDB 31030000), the National Natural Science Foundation of China (32171581 , 31670632 , 31971439), the National Science Foundation of Liaoning Province of China (2021-MS-028). AA is currently supported by Hebei University (Special Project No. 521100221033).

Supporting Information

Fig. S1 Spearman correlations among candidate predictors (the abbreviations of leaf traits were showed in Table S3)

Fig. S2 Distribution of main phyla of phyllosphere microbes (the abbreviations of tree species were shown in Table S1)

Fig. S3 Relative abundances of the dominant phylum and class for bacterial and fungal in the phyllosphere separated according to elevation categories. There were significant differences between communities at different elevations. Abbreviations: $Bacteria_{All}$, all bacteria; $Bacteria_{Endo}$, endophytic bacteria; $Bacteria_{Epip}$, epiphytic bacteria; $Fungi_{All}$, all fungi; $Fungi_{Endo}$, endophytic fungi; $Fungi_{epip}$, epiphytic fungi.

Fig. S4 A conceptual model revealing the expected links of abiotic factors (mean annual temperature) and biotic factors (leaf function traits) on phyllosphere microbial diversity. Abbreviations: $Bacteria_{All}$, all bacteria; $Bacteria_{Endo}$, endophytic bacteria; $Bacteria_{Epip}$, epiphytic bacteria; $Fungi_{All}$, all fungi; $Fungi_{Endo}$, endophytic fungi; $Fungi_{epip}$, epiphytic fungi.

Fig. S5 Effects of mean annual temperature, plant identity(CWM_{MH}), and leaf functional traits on phyllosphere bacterial (a, c, d) and fungal (b, e, f) Shannon's diversity. We present the standardized regression coefficients of model predictors, and the associated 95% confidence intervals. We also present the relative importance of each predictor (expressed as the percentage of total variance). Significance levels are **: $P < 0.01$; ***: $P < 0.001$. Abbreviations: H, Shannon's diversity; MAT, mean annual temperature; MAT^2, the square of mean annual temperature; $bacteria_{All}$, all bacteria; $Bacteria_{Endo}$, endophytic bacteria; $Bacteria_{Epip}$, epiphytic bacteria; $Fungi_{All}$, all fungi; $Fungi_{Endo}$, endophytic fungi; $Fungi_{epip}$, epiphytic fungi; CWM_{MH}, the community-weighted mean of maximum tree height; FT_{PC1}, the first PCA axis on the nine functional traits considered; FT_{PC2}, the second PCA axis.

Figure. S6 Piecewise structural equation models (pSEMs) exploring the direct and indirect effects of mean annual temperature and leaf functional traits on phyllosphere bacterial and fungi Shannon's diversity. Standardized regression coefficients and significance are given (*<0.05, **<0.01). The effect sizes of direct and indirect paths are also presented. Abbreviation: H,

Shannon's diversity; $Bacteria_{All}$, all bacteria; $Bacteria_{Endo}$, endophytic bacteria; $Bacteria_{Epip}$, epiphytic bacteria; $Fungi_{All}$, all fungi; $Fungi_{Endo}$, endophytic fungi; $Fungi_{epip}$, epiphytic fungi; FT_{pc1}, the first PCA axis on the nine functional traits studied; MAT, mean annual temperature.

Figure. S7 Piecewise structural equation models (pSEMs) exploring the effects of mean annual temperature and leaf functional traits on phyllosphere bacterial and fungi richness. Standardized regression coefficients and significance are given (*<0.05, **<0.01). Abbreviation: S, richness; $Bacteria_{All}$, all bacteria; $Bacteria_{Endo}$, endophytic bacteria; $Bacteria_{Epip}$, epiphytic bacteria; $Fungi_{All}$, all fungi; $Fungi_{Endo}$, endophytic fungi; $Fungi_{epip}$, epiphytic fungi; FT_{pc1}, the first PCA axis on the nine functional traits studied; MAT, mean annual temperature.

Figure. S8 Piecewise structural equation models (pSEMs) exploring the effects of mean annual temperature and leaf functional traits on phyllosphere bacterial and fungi Shannon's diversity. Standardized regression coefficients and significance are given (*<0.05, **<0.01). Abbreviation: H, Shannon's diversity; $Bacteria_{All}$, all bacteria; $Bacteria_{Endo}$, endophytic bacteria; $Bacteria_{Epip}$, epiphytic bacteria; $Fungi_{All}$, all fungi; $Fungi_{Endo}$, endophytic fungi; $Fungi_{epip}$, epiphytic fungi; FT_{pc1}, the first PCA axis on the nine functional traits studied; MAT, mean annual temperature.

Figure. S9 Heatmap that shows relationship between plant functional traits and specific microbial taxa (in the phyla level).

Table S1 Summary of the main characteristics of sampling sites along an elevational gradient on Changbai Mountain.

Table S2 Geographic information of the studied sites.

Table S3 Functional traits and their functions.

Table S4 Loadings of the Principal Component Analysis for trait values.

Table S5 AIC value for predicting the relationship between phyllosphere microbial richness and elevation(elevation^2). Bold represents the optimal model based on AIC. *: $P < 0.01$.

Table S6 AIC value for predicting the relationship between phyllosphere microbial Shannon index and elevation (elevation^2). Bold represents the optimal model based on AIC. *: $P < 0.01$.

Table S7 The direct, indirect, and total standardized effects of mean annual temperature and leaf functional traits on phyllosphere bacterial and fungal richness derived from the pierce structural equation models. Models are presented in Fig. 4. Only significant effects are shown.

Table S8 The direct, indirect, and total standardized effects of mean annual temperature and leaf functional traits on phyllosphere bacterial and fungal Shannon index derived from the pierce structural equation models. Models are presented in Fig. S5. Only significant effects are shown.

Figure legends

Figure 1. The geographical position of the Changbai Mountain in north-east China (a), the location of study sites with the respective dominant forests (pictures) along an elevational gradient from 800 m to 1950 m above sea level (b), and the design of the study plot for samples collections (c).

Figure 2. The richness of phyllosphere bacteria (a, b) and phyllosphere fungi (c, d) along the studied elevational gradient. Abbreviations: S, richness; H, Shannon index;

548 $Bacteria_{All}$, all bacteria; $Bacteria_{Endo}$, endophytic bacteria; $Bacteria_{Epip}$, epiphytic
549 bacteria; $Fungi_{All}$, all fungi; $Fungi_{Endo}$, endophytic fungi; $Fungi_{epip}$, epiphytic fungi.

550 **Figure 3.** Effects of mean annual temperature, tree functional identity (CWM_{MH}), and
551 leaf functional traits on phyllosphere bacterial (a, c, d) and fungal (b, e, f) richness. We
552 present the standardized regression coefficients of model predictors and the associated
553 95% confidence intervals. We also present the relative importance of each predictor
554 (expressed as the percentage of total variance). Significance levels are **: $P < 0.01$;
555 ***: $P < 0.001$. Abbreviations: S, richness; MAT, mean annual temperature; MAT^2,
556 the square of mean annual temperature; $Bacteria_{All}$, all bacteria; $Bacteria_{Endo}$,
557 endophytic bacteria; $Bacteria_{Epip}$, epiphytic bacteria; $Fungi_{All}$, all fungi; $Fungi_{Endo}$,
558 endophytic fungi; $Fungi_{epip}$, epiphytic fungi; FT_{PC1}, the first PCA axis on the nine
559 functional traits considered; FT_{PC2}, the second PCA axis.

560

561 **Figure 4.** Piecewise structural equation models (pSEMs) exploring the direct and
562 indirect effects of mean annual temperature and leaf functional traits on phyllosphere
563 bacterial and fungi richness. Standardized regression coefficients and significance are
564 given (*<0.05, **<0.01). The effect sizes of direct and indirect paths are also presented.
565 Abbreviation: S, richness; $Bacteria_{All}$, all bacteria; $Bacteria_{Endo}$, endophytic bacteria;
566 $Bacteria_{Epip}$, epiphytic bacteria; $Fungi_{All}$, all fungi; $Fungi_{Endo}$, endophytic fungi;
567 $Fungi_{epip}$, epiphytic fungi; FT_{pc1}, the first PCA axis on the nine functional traits studied;

MAT, mean annual temperature.

571 **Fig. 1**

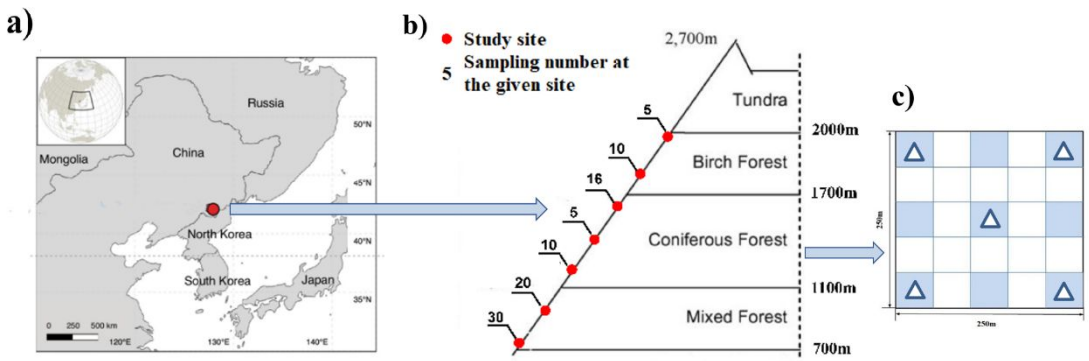

572

573

574

575 **Fig. 2**

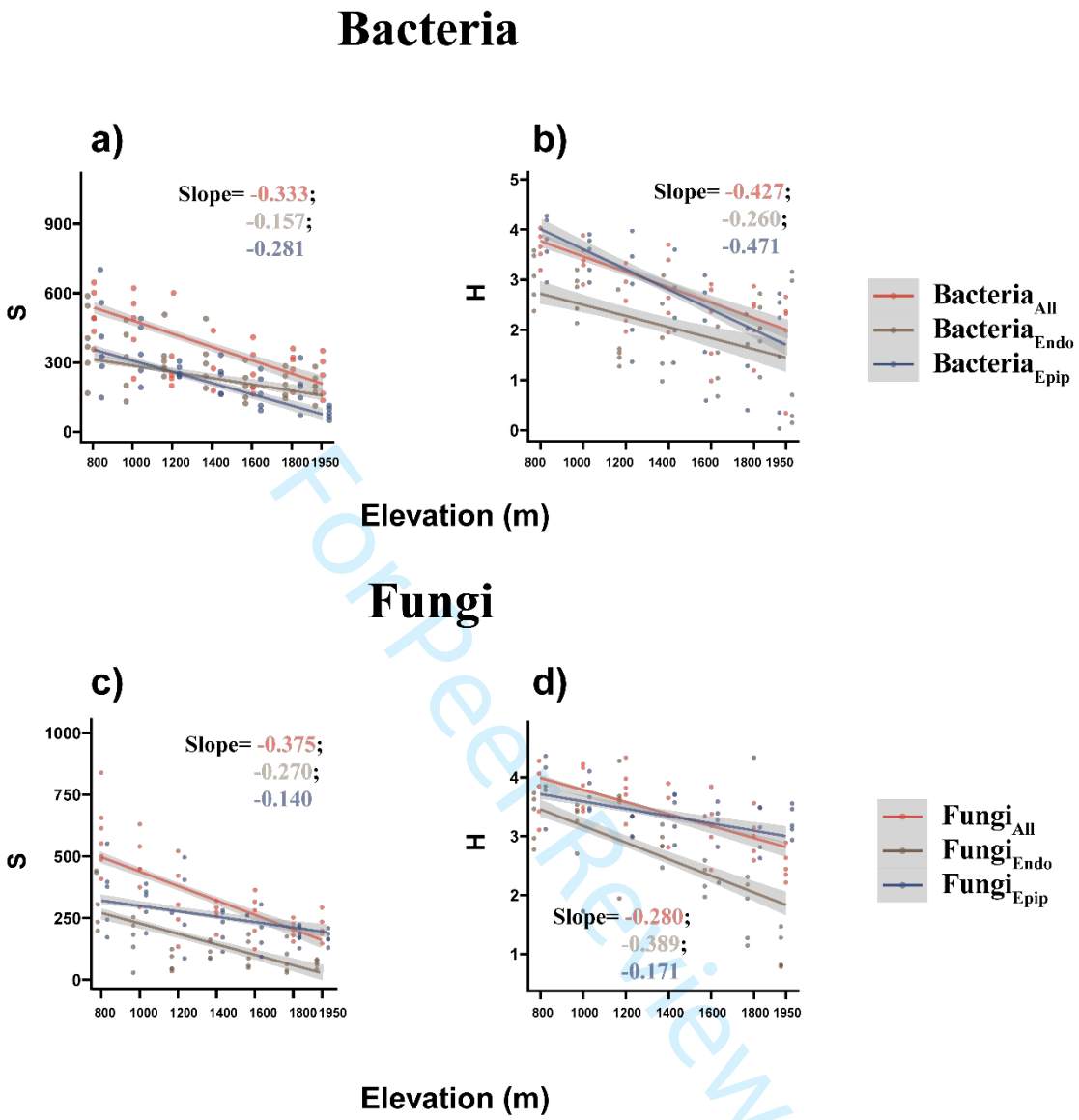

576

577

578

579

Fig. 3

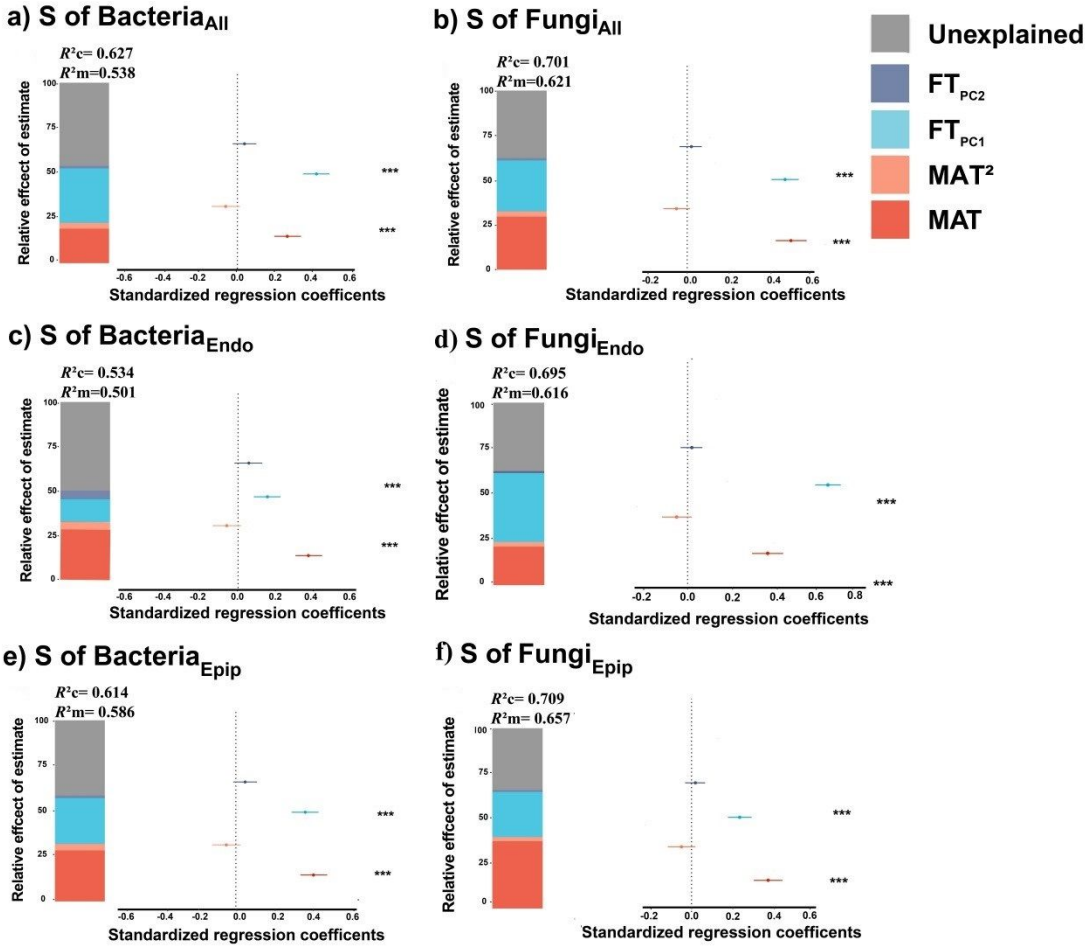

584 **Fig. 4**

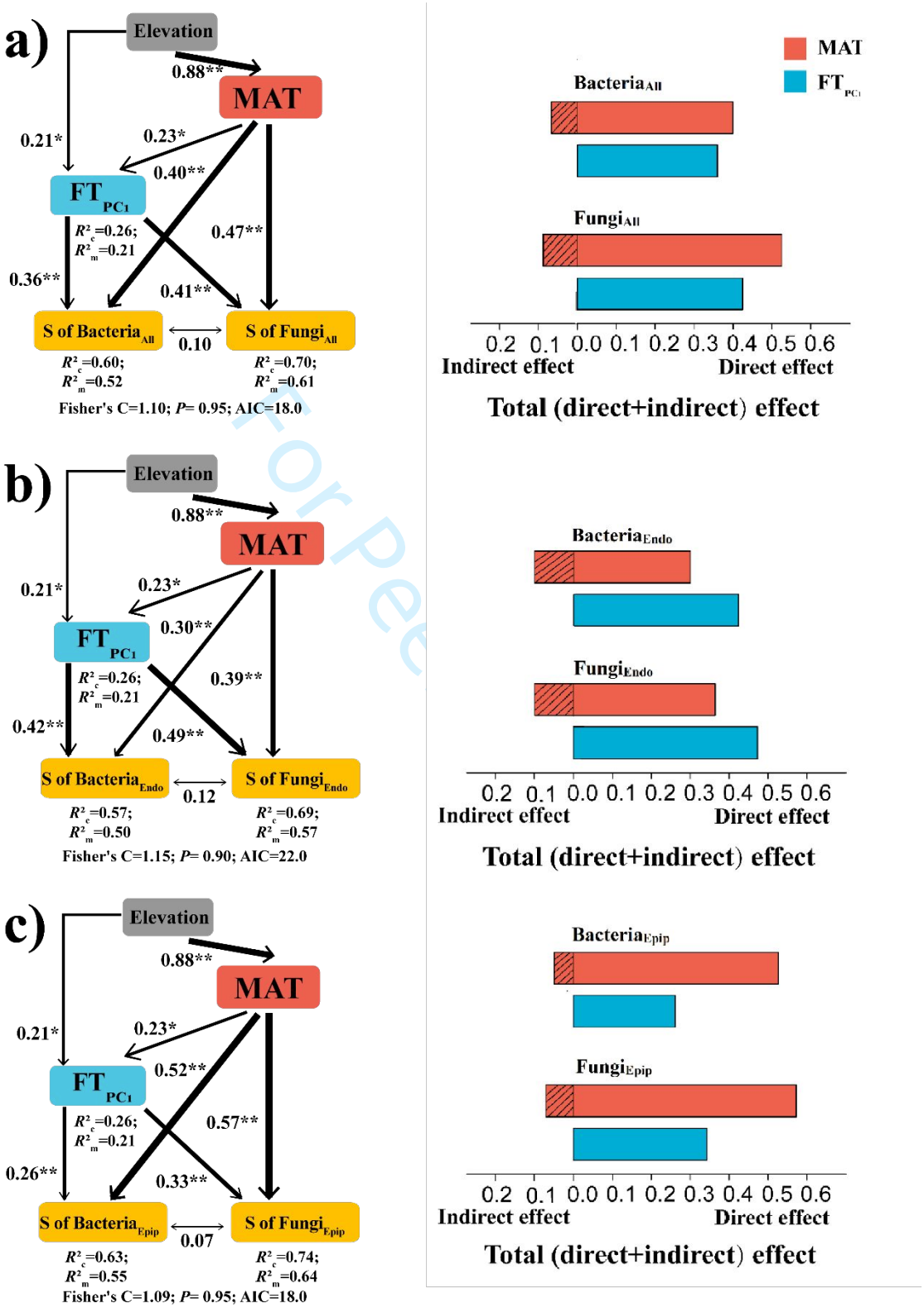

585

586

587

References

Agler, M. T., Ruhe, J., Kroll, S., Morhenn, C., Kim, S. T., Weigel, D., & Kemen, E. M. (2016). Microbial hub taxa link host and abiotic factors to plant microbiome variation. *Plos Biology, 14*(1), e1002352. doi:https://doi.org/10.1371/journal.pbio.1002352

Bahram, M., Hildebrand, F., Forslund, S., Anderson, J., Soudzilovskaia, N., Bodegom, P., . . . Bork, P. (2018). Structure and function of the global topsoil microbiome. *Nature, 560*, 233-237. doi:https://doi.org/10.1038/s41586-018-0386-6

Bartoń, K. (2020). MuMIn: Multi-model inference. *R package version 1.43.17. https://CRAN.R-project.org/package=MuMIn*.

Bodenhausen, N., Horton, M. W., & Bergelson, J. (2013). Bacterial communities associated with the leaves and the roots of *Arabidopsis thaliana*. *Plos One, 8*(2), e56329. doi:https://doi.org/10.1371/journal.pone.0056329

Boer, W. d., Folman, L. B., Summerbell, R. C., & Boddy, L. (2005). Living in a fungal world: impact of fungi on soil bacterial niche development. *FEMS Microbiology Reviews, 29*(4), 795-811. doi:https://doi.org/10.1016/j.femsre.2004.11.005

Bolnick, D., Amarasekare, P., Araújo, M., Bürger, R., Levine, J., Novak, M., . . . Vasseur, D. (2011). Why intraspecific trait variation matters in community ecology. *Trends in Ecology and Evolution, 26*, 183-192. doi:https://doi.org/10.1016/j.tree.2011.01.009

Brown, J. H., Gillooly, J. F., Allen, A. P., Savage, V. M., & West, G. B. (2004). Toward a metabolic theory of ecology. *Ecology, 85*(7), 1771-1789. doi: https://doi.org/10.1890/03-9000

Bruno, J. F., Stachowicz, J. J., & Bertness, M. D. (2003). Inclusion of facilitation into ecological theory. *Trends in Ecology and Evolution, 18*(3), 119-125. doi:https://doi.org/10.1016/S0169-5347(02)00045-9

Bryant, J. A., Lamanna, C., Morlon, H., Kerkhoff, A. J., Enquist, B. J., & Green, J. L. (2008). Microbes on mountainsides: Contrasting elevational patterns of bacterial and plant diversity. *Proceedings of the National Academy of Sciences of the United States of America, 105*, 11505-11511. doi:https://doi.org/10.1073/pnas.0801920105

Bulgarelli, D., Garrido-Oter, R., Münch, P. C., Weiman, A., Dröge, J., Pan, Y., . . . microbe. (2015). Structure and function of the bacterial root microbiota in wild and domesticated barley. *Cell Host and Microbe, 17*(3), 392-403. doi:https://doi.org/10.1016/j.chom.2015.01.011

Bulgarelli, D., Rott, M., Schlaeppi, K., Ver Loren van Themaat, E., Ahmadinejad, N., Assenza, F., . . . Schmelzer, E. (2012). Revealing structure and assembly cues for Arabidopsis root-inhabiting bacterial microbiota. *Nature, 488*(7409), 91-95. doi:https://doi.org/10.1038/nature11336

Butterfield, B. J., Cavieres, L. A., Callaway, R. M., Cook, B. J., Kikvidze, Z., Lortie, C. J., . . . Brooker, R. W. (2013). Alpine cushion plants inhibit the loss of phylogenetic diversity in severe environments. *Ecol Lett, 16*(4), 478-486. doi:https://doi.org/10.1111/ele.12070

Carvalho, S. D., & Castillo, J. A. (2018). Influence of light on plant-phyllosphere interaction. *Frontiers in Plant Science, 9*, 1482. doi:https://doi.org/10.3389/fpls.2018.01482

Cavieres, L. A., Brooker, R. W., Butterfield, B. J., Cook, B. J., Kikvidze, Z., Lortie, C. J., . . . Callaway, R. M. (2014). Facilitative plant interactions and climate simultaneously drive alpine plant diversity. *Ecol Lett, 17*(2), 193-202. doi:https://doi.org/10.1111/ele.12217

Chave, J., Coomes, D., Jansen, S., Lewis, S. L., Swenson, N. G., & Zanne, A. E. (2009). Towards a worldwide wood economics spectrum. *Ecol Lett, 12*(4), 351-366. doi:https://doi.org/10.1111/j.1461-0248.2009.01285.x

Cordier, T., Robin, C., Capdevielle, X., Olivier, F., Desprez-Loustau, M.-L., & Vacher, C. (2012). The composition of phyllosphere fungal assemblages of European beech (*Fagus sylvatica*) varies significantly along an elevation gradient. *New Phytologist, 196*(2), 510-519. doi:https://doi.org/10.1111/j.1469-8137.2012.04284.x

Devictor, V., Clavel, J., Julliard, R., Lavergne, S., Mouillot, D., Thuiller, W., . . . Mouquet, N. (2010). Defining and measuring ecological specialization. *Journal of Applied Ecology, 47*(1), 15-25. doi:https://doi.org/10.1111/j.1365-2664.2009.01744.x

Diaz, S., Kattge, J., Cornelissen, J. H. C., Wright, I. J., Lavorel, S., Dray, S., . . . Gorne, L. D. (2016). The global spectrum of plant form and function. *Nature, 529*(7585), 167-171. doi:https://doi.org/10.1038/nature16489

Díaz, S., Lavorel, S., de Bello, F., Quétier, F., Grigulis, K., & Robson, T. M. (2007). Incorporating plant functional diversity effects in ecosystem service assessments. *Proceedings of the National Academy of Sciences of the United States of America, 104*(52), 20684-20689. doi:https://doi.org/10.1073/pnas.0704716104

Duclos, T. R., DeLuca, W. V., & King, D. I. (2019). Direct and indirect effects of climate on bird

abundance along elevation gradients in the Northern Appalachian mountains. *Diversity and Distributions, 25*(11), 1670-1683. doi:https://doi.org/10.1111/ddi.12968

Edgar, R. C. (2013). UPARSE: highly accurate OTU sequences from microbial amplicon reads. *Nature Methods, 10*(10), 996-998. doi:https://doi.org/10.1038/nmeth.2604

Flynn, D. F., Mirotchnick, N., Jain, M., Palmer, M. I., & Naeem, S. (2011). Functional and phylogenetic diversity as predictors of biodiversity–ecosystem-function relationships. *Ecology, 92*(8), 1573-1581. doi:https://doi.org/10.1890/10-1245.1

Geml, J., Arnold, A. E., Semenova-Nelsen, T. A., Nouhra, E. R., Drechsler-Santos, E. R., Goes-Neto, A., . . . Lutzoni, F. (2022). Community dynamics of soil-borne fungal communities along elevation gradients in neotropical and palaeotropical forests. *Molecular Ecology, 31*(7), 2044-2060. doi:https://doi.org/10.1111/mec.16368

Giangacomo, C., Mohseni, M., Kovar, L., & Wallace, J. G. (2021). Comparing DNA extraction and 16S rRNA gene amplification methods for plant-associated bacterial communities. *Phytobiomes Journal, 5*(2), 190-201. doi:https://doi.org/10.1094/PBIOMES-07-20-0055-R

Gillooly, J. F., Brown, J. H., West, G. B., Savage, V. M., & Charnov, E. L. (2001). Effects of size and temperature on metabolic rate. *Science, 293*(5538), 2248-2251. doi:https://doi.org/10.1126/science.1061967

Gomes, T., Pereira, J., Benhadi-Marín, J., Lino-Neto, T., & Baptista, P. (2018). Endophytic and epiphytic phyllosphere fungal communities are shaped by different environmental factors in a Mediterranean ecosystem. *Microbial Ecology, 76*(3), 668-679.

doi:https://doi.org/10.1007/s00248-018-1161-9

Götzenberger, L., de Bello, F., Bråthen, K. A., Davison, J., Dubuis, A., Guisan, A., . . . Zobel, M. (2012). Ecological assembly rules in plant communities—approaches, patterns and prospects. *Biological Reviews, 87*(1), 111-127. doi:https://doi.org/10.1111/j.1469-185X.2011.00187.x

Graham, C. H., Parra, J. L., Rahbek, C., & McGuire, J. A. (2009). Phylogenetic structure in tropical hummingbird communities. *Proceedings of the National Academy of Sciences of the United States of America, 106*, 19673-19678. doi:https://doi.org/10.1073/pnas.0901649106

Gross, N., Börger, L., Morales, I., Le Bagousse-Pinguet, Y., Quero, J., Garcia-Gomez, M., . . . Maestre, F. (2013). Uncovering multiscale effects of aridity and biotic interactions on the functional structure of Mediterranean shrubland. *Journal of Ecology, 101*, 637-649. doi:https://doi.org/10.1111/1365-2745.12063

Grytnes, J. A., & Beaman, J. H. (2006). Elevational species richness patterns for vascular plants on Mount Kinabalu, Borneo. *Journal Of Biogeography, 33*(10), 1838-1849. doi:https://doi.org/10.1111/j.1365-2699.2006.01554.x

Guo, Q., Kelt, D., Sun, Z., Liu, H., Hu, L., Ren, H., & Wen, J. (2013). Global variation in elevational diversity patterns. *Scientific Reports, 3*, 3007. doi:https://doi.org/10.1038/srep03007

Harms, K., Condit, R., Hubbell, S., & Foster, R. (2001). Habitat associations of trees and shrubs in a 50-ha Neotropical forest plot. *Journal of Ecology, 89*, 947-959.

doi:https://doi.org/10.1046/j.0022-0477.2001.00615.x

Herrmann, M., Geesink, P., Richter, R., & Küsel, K. (2021). Canopy position has a stronger effect than tree species identity on phyllosphere bacterial diversity in a floodplain hardwood forest. *Microbial Ecology, 81*(1), 157-168. doi:https://doi.org/10.1007/s00248-020-01565-y

Inácio, J., Pereira, P., Carvalho, d. M., Fonseca, A., Amaral-Collaco, M., & Spencer-Martins, I. (2002). Estimation and diversity of phylloplane mycobiota on selected plants in a mediterranean–type ecosystem in Portugal. *Microbial Ecology, 44*(4), 344-353.

Jennings, D. (1987). Translocation of solutes in fungi. *Biological Reviews, 62*(3), 215-243. doi:https://doi.org/10.1111/j.1469-185X.1987.tb00664.x

Jia, T., Yao, Y., Guo, T., Wang, R., & Chai, B. (2020). Effects of plant and soil characteristics on phyllosphere and rhizosphere fungal communities during plant development. *Frontiers in Microbiology, 11*, doi: 10.3389/fmicb.2020.556002. doi:https://doi.org/10.3389/fmicb.2020.556002

Jiao, S., Peng, Z., Qi, J., Gao, J., Wei, G., & Stegen, J. C. (2021). Linking bacterial-fungal relationships to microbial diversity and soil nutrient cycling. *Msystems, 6*(2), e01052-01020. doi:https://doi.org/10.1128/mSystems.01052-20

Kembel, S. W., & Mueller, R. C. (2014). Plant traits and taxonomy drive host associations in tropical phyllosphere fungal communities. *Botany, 92*(4), 1-10. doi:https://doi.org/10.1139/cjb-2013-0194

Kembel, S. W., O'Connor, T. K., Arnold, H. K., Hubbell, S. P., Wright, S. J., & Green, J. L.

(2014). Relationships between phyllosphere bacterial communities and plant functional traits in a neotropical forest. *Proceedings of the National Academy of Sciences of the United States of America, 111*(38), 13715-13720. doi:https://doi.org/10.1073/pnas.1216057111

Körner, C. (2000). Why are there global gradients in species richness? Mountains might hold the answer. *Trends in Ecology and Evolution, 15*, 513-514. doi:https://doi.org/10.1016/S0169-5347(00)02004-8

Kotilinek, M., Hiiesalu, I., Kosnar, J., Smilauerov, M., Smilauer, P., Altman, J., . . . Dolezal, J. (2017). Fungal root symbionts of high-altitude vascular plants in the Himalayas. *Scientific Reports, 7*, 1-14. doi:https://doi.org/10.1038/s41598-017-06938-x

Kraft, N., Crutsinger, G., Forrestel, E., & Emery, N. (2014). Functional trait differences and the outcome of community assembly: An experimental test with vernal pool annual plants. *Oikos, 123*(11), 1391-1399. doi:https://doi.org/10.1111/oik.01311

Le Bagousse-Pinguet, Y., Börger, L., Quero, J., García-Gómez, M., Soriano, S., Maestre, F., & Gross, N. (2015). Traits of neighbouring plants and space limitation determine intraspecific trait variability in semi-arid shrublands. *Journal of Ecology, 103*(6), 1647-1657. doi:https://doi.org/10.1111/1365-2745.12480

Le Bagousse-Pinguet, Y., Gross, N., Maestre, F. T., Maire, V., de Bello, F., Fonseca, C. R., . . . Liancourt, P. (2017). Testing the environmental filtering concept in global drylands. *Journal of Ecology, 105*(4), 1058-1069. doi:https://doi.org/10.1111/1365-2745.12735

Le Bagousse-Pinguet, Y., Liancourt, P., Götzenberger, L., de Bello, F., Altman, J., Brozova, V.,

. . . Dolezal, J. (2018). A multi-scale approach reveals random phylogenetic patterns at the edge of vascular plant life. *Perspectives in Plant Ecology, Evolution and Systematics, 30*, 22-30. doi:https://doi.org/10.1016/j.ppees.2017.https://doi.org/10.002

Le Bagousse-Pinguet, Y., Soliveres, S., Gross, N., Torices, R., Berdugo, M., & Maestre, F. T. (2019). Phylogenetic, functional, and taxonomic richness have both positive and negative effects on ecosystem multifunctionality. *Proceedings of the National Academy of Sciences of the United States of America, 116*(17), 8419-8424. doi:https://doi.org/10.1073/pnas.1815727116

Lefcheck, J. S. (2016). PIECEWISESEM: Piecewise structural equation modelling in R for ecology, evolution, and systematics. *Methods in Ecology and Evolution, 7*(5), 573-579. doi:https://doi.org/10.1111/2041-210x.12512

Leff, J., Bardgett, R., Wilkinson, A., Jackson, B., Pritchard, W., De Long, J., . . . Fierer, N. (2018). Predicting the structure of soil communities from plant community taxonomy, phylogeny, and traits. *The ISME journal, 12*(7), 1794-1805. doi:https://doi.org/10.1038/s41396-018-0089-x

Leveau, J. H. J. (2019). A brief from the leaf: latest research to inform our understanding of the phyllosphere microbiome. *Current Opinion in Microbiology, 49*, 41-49. doi:https://doi.org/10.1016/j.mib.2019.https://doi.org/10.002

Liancourt, P., Song, X., Macek, M., Santrucek, J., & Dolezal, J. (2020). Plant's-eye view of temperature governs elevational distributions. *Global Change Biology, 26*(7), 4094-4103. doi:https://doi.org/10.1111/gcb.15129

Liu, H., Brettell, L. E., & Singh, B. (2020). Linking the phyllosphere microbiome to plant health. *Trends in Plant Science, 25*(9), 841-844. doi:https://doi.org/10.1016/j.tplants.2020.06.003

Lundberg, D. S., Lebeis, S. L., Paredes, S. H., Yourstone, S., Gehring, J., Malfatti, S., . . . Rio, T. G. d. (2012). Defining the core *Arabidopsis thaliana* root microbiome. *Nature, 488*(7409), 86-90. doi:https://doi.org/10.1038/nature11237

Machac, A., Janda, M., Dunn, R. R., & Sanders, N. J. (2011). Elevational gradients in phylogenetic structure of ant communities reveal the interplay of biotic and abiotic constraints on diversity. *Ecography, 34*(3), 364-371. doi:https://doi.org/10.1111/j.1600-0587.2010.06629.x

Mao, Z., Corrales, A., Zhu, K., Yuan, Z., Lin, F., Ye, J., . . . Wang, X. (2019). Tree mycorrhizal associations mediate soil fertility effects on forest community structure in a temperate forest. *New Phytologist, 223*(1), 475-486. doi:https://doi.org/10.1111/nph.15742

Martínez-García, L. B., Richardson, S. J., Tylianakis, J. M., Peltzer, D. A., & Dickie, I. A. (2015). Host identity is a dominant driver of mycorrhizal fungal community composition during ecosystem development. *New Phytologist, 205*(4), 1565-1576.

Michaletz, S. T., Weiser, M. D., Zhou, J., Kaspari, M., Helliker, B. R., & Enquist, B. J. (2015). Plant thermoregulation: energetics, trait-environment interactions, and carbon economics. *Trends in Ecology and Evolution, 30*(12), 714-724. doi:https://doi.org/10.1016/j.tree.2015.09.006

Mina, D., Pereira, J., Lino-Neto, T., & Baptista, P. (2020). Epiphytic and endophytic bacteria on

olive tree phyllosphere: exploring tissue and cultivar effect. *Microbial Ecology, 80*, 145–157. doi:https://doi.org/10.1007/s00248-020-01488-8

Nottingham, A. T., Fierer, N., Turner, B. L., Whitaker, J., Ostle, N. J., McNamara, N. P., . . . Meir, P. (2018). Microbes follow Humboldt: temperature drives plant and soil microbial diversity patterns from the Amazon to the Andes. *Ecology, 99*(11), 2455-2466. doi:https://doi.org/10.1002/ecy.2482

Pérez-Harguindeguy, N., Díaz, S., Garnier, E., Lavorel, S., Poorter, H., Jaureguiberry, P., . . . Gurvich, D. (2013). New handbook for standardised measurement of plant functional traits worldwide. *Australian Journal of botany, 61*(3), 167-234.

Rahbek, C. (1995). The elevational gradient of species richness: a uniform pattern? *Ecography, 18*(2), 200-205.

Rahbek, C., Borregaard, M. K., Colwell, R. K., Dalsgaard, B., Holt, B. G., Morueta-Holme, N., . . . Fjeldså, J. (2019). Humboldt's enigma: What causes global patterns of mountain biodiversity? *Science, 365*(6458), 1108-1113. doi:https://doi.org/10.1126/science.aax0149

Rehakova, K., Chlumska, Z., & Dolezal, J. (2011). Soil cyanobacterial and microalgal diversity in dry mountains of Ladakh, NW Himalaya, as related to site, altitude, and vegetation. *Microbial Ecology, 62*(2), 337-346. doi:https://doi.org/10.1007/s00248-011-9878-8

Sanders, N. J. (2002). Elevational gradients in ant species richness: area, geometry, and Rapoport's rule. *Ecography, 25*(1), 25-32. doi:https://doi.org/10.1034/j.1600-0587.2002.250104.x

Shao, G., Schall, P., & Weishampel, J. F. (1994). Dynamic simulations of mixed broadleaved-Pinus koraiensis forests in the Changbaishan Biosphere Reserve of China. *Forest Ecology and Management, 70*(1-3), 169-181.

Shen, C., Liang, W., Shi, Y., Lin, X., Zhang, H., Wu, X., . . . Chu, H. (2014). Contrasting elevational diversity patterns between eukaryotic soil microbes and plants. *Ecology, 95*(11), 3190-3202. doi:https://doi.org/10.1890/14-0310.1

Shen, C., Xiong, J., Zhang, H., Feng, Y., Lin, X., Li, X., . . . Chu, H. (2013). Soil pH drives the spatial distribution of bacterial communities along elevation on Changbai Mountain. *Soil Biology and Biochemistry, 57*, 204-211. doi:https://doi.org/10.1016/j.soilbio.2012.07.013

Shipley, B. (2009). Confirmatory path analysis in a generalized multilevel context. *Ecology, 90*(2), 363-368. doi:https://doi.org/10.1890/08-1034.1

Shrestha, N., Su, X., Xu, X., & Wang, Z. (2018). The drivers of high *Rhododendron* diversity in south-west China: Does seasonality matter? *Journal Of Biogeography, 45*(2), 438-447. doi:https://doi.org/10.1111/jbi.13136

Smith, M. A., Hallwachs, W., & Janzen, D. H. (2014). Diversity and phylogenetic community structure of ants along a Costa Rican elevational gradient. *Ecography, 37*(8), 720-731. doi:https://doi.org/10.1111/j.1600-0587.2013.00631.x

Stone, R. (2006). A threatened nature reserve breaks down Asian borders. *Science, 313*(5792), 1379-1380. doi:https://doi.org/10.1126/science.313.5792.1379

Vacher, C., Cordier, T., & Vallance, J. (2016). Phyllosphere fungal communities differentiate

more thoroughly than bacterial communities along an elevation gradient. *Microbial Ecology, 72*(1), 1-3. doi:https://doi.org/10.1007/s00248-016-0742-8

Vacher, C., Hampe, A., Porté, A. J., Sauer, U., Compant, S., & Morris, C. E. (2016). The phyllosphere: Microbial jungle at the plant-climate interface. *Annual Review of Ecology, Evolution, and Systematics, 47*(1), 1-24. doi:https://doi.org/10.1146/annurev-ecolsys-121415-032238

Violle, C., Enquist, B., McGill, B., Jiang, L., Albert, C., Hulshof, C., . . . Messier, J. (2012). The return of the variance: Intraspecific variability in community ecology. *Trends in Ecology and Evolution, 27*, 244-252. doi:https://doi.org/10.1016/j.tree.2011.11.014

Von Humboldt, A., & Bonpland, A. (1805). Essai sur la géographie des plantes (Chez Levrault, Schoell et compagnie, libraires, Paris).

Vorholt, J. A. (2012). Microbial life in the phyllosphere. *Nature Reviews Microbiology, 10*(12), 828-840. doi:https://doi.org/10.1038/nrmicro2910

Wang, F., Harindintwali, J. D., Yuan, Z., Min, W., Wang, F., Li, S., . . . Chen, J. (2021). Technologies and perspectives for achieving carbon neutrality. *The Innovation, 2*(4), 100-180. doi:https://doi.org/10.1016/j.xinn.2021.100180

Wang, J., Meier, S., Soininen, J., Casamayor, E. O., Pan, F., Tang, X., . . . Shen, J. (2017). Regional and global elevational patterns of microbial species richness and evenness. *40*(3), 393-402. doi:https://doi.org/10.1111/ecog.02216

Wang, Q., Garrity, G. M., Tiedje, J. M., & Cole, J. R. (2007). Naive Bayesian classifier for rapid assignment of rRNA sequences into the new bacterial taxonomy. *Applied and*

Environmental Microbiology *73*(16), 5261-5267. doi:https://doi.org/10.1128/aem.00062-07

Wang, X., Swenson, N. G., Wiegand, T., Wolf, A., Howe, R., Lin, F., . . . Bai, X. (2013). Phylogenetic and functional diversity area relationships in two temperate forests. *Ecography, 36*(8), 883-893. doi:https://doi.org/10.1111/j.1600-0587.2012.00011.x

Wang, X., Wiegand, T., Kraft, N. J., Swenson, N. G., Davies, S. J., Hao, Z., . . . Mi, X. (2016). Stochastic dilution effects weaken deterministic effects of niche-based processes in species rich forests. *Ecology, 97*(2), 347-360. doi:https://doi.org/10.1890/14-2357.1

Wei, T., Simko, V., Levy, M., Xie, Y., Jin, Y., & Zemla, J. (2017). Package 'corrplot'. *Statistician, 56*(316), e24.

Wei, Y., Lan, G., Wu, Z., Chen, B., Quan, F., Li, M., . . . Du, H. (2022). Phyllosphere fungal communities of rubber trees exhibited biogeographical patterns, but not bacteria. *Environmental microbiology, 24*, 3777-3790. doi:https://doi.org/10.1111/1462-2920.15894

Weiher, E., Clarke, G. D. P., & Keddy, P. A. (1998). Community assembly rules, morphological dispersion, and the coexistence of plant species. *Oikos, 81*(2), 309-322. doi:https://doi.org/10.2307/3547051

Wright, I., Reich, P., Westoby, M., Ackerly, D., Baruch, Z., Bongers, F., . . . Villar, R. (2004). The world-wide leaf economics spectrum. *Nature, 21*(428), 821-827. doi:https://doi.org/10.1111/j.1466-8238.2012.00761.x

Yang, H. (1985). Distribution patterns of dominant tree species on northern slope of Changbai

Mountain. *Research Forest Ecosystem, 5*, 1-14.

Yang, T., Tedersoo, L., Soltis, P., Soltis, D., Gilbert, J., Sun, M., . . . Chu, H. (2019). Phylogenetic imprint of woody plants on the soil mycobiome in natural mountain forests of eastern China. *The ISME journal, 13*, 686-697. doi:https://doi.org/10.1038/s41396-018-0303-x

Yang, X., Wu, J., Chen, X., Ciais, P., Maignan, F., Yuan, W., . . . Wright, S. J. (2021). A comprehensive framework for seasonal controls of leaf abscission and productivity in evergreen, broadleaved tropical and subtropical forests. *The Innovation, 2*, 100154. doi:https://doi.org/10.1016/j.xinn.2021.100154

Yao, H., Sun, X., He, C., Li, X.-C., & Guo, L.-D. (2020). Host identity is more important in structuring bacterial epiphytes than endophytes in a tropical mangrove forest. *Fems Microbiology Ecology, 96*(4), fiaa038. doi:https://doi.org/10.1093/femsec/fiaa038

Yao, H., Sun, X., He, C., Maitra, P., Li, X.-C., & Guo, L.-D. (2019). Phyllosphere epiphytic and endophytic fungal community and network structures differ in a tropical mangrove ecosystem. *Microbiome, 7*(1), 1-15. doi:https://doi.org/10.1186/s40168-019-0671-0

Yuan, Z., Ali, A., Loreau, M., Ding, F., Liu, S., Sanaei, A., . . . Le Bagousse-Pinguet, Y. (2021). Divergent above- and below-ground biodiversity pathways mediate disturbance impacts on temperate forest multifunctionality. *Global Change Biology, 27*(12), 2883-2894. doi:https://doi.org/10.1111/gcb.15606

Yuan, Z., Ali, A., Ruiz-Benito, P., Jucker, T., Mori, A., Wang, S., . . . Loreau, M. (2020). Above - and below - ground biodiversity jointly regulate temperate forest multifunctionality

along a local - scale environmental gradient. *Journal of Ecology, 108*, 2012– 2024. doi:https://doi.org/10.1111/1365-2745.13378

Yuan, Z., Gazol, A., Lin, F., Ye, J., Shi, S., Wang, X., . . . Hao, Z. (2013). Soil organic carbon in an old-growth temperate forest: spatial pattern, determinants and bias in its quantification. *Geoderma, 195*, 48-55. doi:https://doi.org/10.1016/j.geoderma.2012.11.008

Zhang, J.-T., Xiao, J., & Li, L. (2015). Variation of plant functional diversity along a disturbance gradient in mountain meadows of the Donglingshan reserve, Beijing, China. *Russian Journal of Ecology, 46*(2), 157-166. doi:https://doi.org/10.1134/s1067413615020058

Zhao, W. L., Chen, Y. J., Brodribb, T. J., & Cao, K. F. (2016). Weak co-ordination between vein and stomatal densities in 105 angiosperm tree species along altitudinal gradients in Southwest China. *Functional Plant Biology, 43*(12), 1126-1133. doi:https://doi.org/10.1071/fp16012

Zhu, Y. G., Xiong, C., Wei, Z., Chen, Q. L., Ma, B., Zhou, S. Y. D., . . . Duan, G. L. J. N. P. (2021). Impacts of global change on phyllosphere microbiome. *New Phytologist, 234*, 1977-1986. doi:https://doi.org/10.1111/nph.17928

Supporting information

Fig. S1 Spearman correlations among candidate predictors (the abbreviations of leaf traits were showed in Table S3)

Fig. S2 Distribution of main phyla of phyllosphere microbes (the abbreviations of tree species were shown in Table S1)

Fig. S3 Relative abundances of the dominant phylum and class for bacterial and fungal in the phyllosphere separated according to elevation categories. There were significant differences between communities at different elevations. Abbreviations: $Bacteria_{All}$, all bacteria; $Bacteria_{Endo}$, endophytic bacteria; $Bacteria_{Epip}$, epiphytic bacteria; $Fungi_{All}$, all fungi; $Fungi_{Endo}$, endophytic fungi; $Fungi_{epip}$, epiphytic fungi.

Fig. S4 A conceptual model revealing the expected links of abiotic factors (mean annual temperature) and biotic factors (leaf function traits) on phyllosphere microbial diversity. Abbreviations: $Bacteria_{All}$, all bacteria; $Bacteria_{Endo}$, endophytic bacteria; $Bacteria_{Epip}$, epiphytic bacteria; $Fungi_{All}$, all fungi; $Fungi_{Endo}$, endophytic fungi; $Fungi_{epip}$, epiphytic fungi.

Fig. S5 Effects of mean annual temperature, plant identity(CWM_{MH}), and leaf functional traits on phyllosphere bacterial (a, c, d) and fungal (b, e, f) Shannon's diversity. We present the standardized regression coefficients of model predictors, and the associated 95% confidence intervals. We also present the relative importance of each predictor (expressed as the percentage of total variance). Significance levels are **: $P < 0.01$; ***: $P < 0.001$. Abbreviations: H, Shannon's diversity; MAT, mean annual temperature; MAT^2, the square of mean annual temperature; $bacteria_{All}$, all bacteria; $Bacteria_{Endo}$, endophytic bacteria; $Bacteria_{Epip}$, epiphytic bacteria; $Fungi_{All}$, all fungi; $Fungi_{Endo}$, endophytic fungi; $Fungi_{epip}$, epiphytic fungi; CWM_{MH}, the

community-weighted mean of maximum tree height; FT_{PC1}, the first PCA axis on the nine functional traits considered; FT_{PC2}, the second PCA axis.

Figure. S6 Piecewise structural equation models (pSEMs) exploring the direct and indirect effects of mean annual temperature and leaf functional traits on phyllosphere bacterial and fungi Shannon's diversity. Standardized regression coefficients and significance are given (*<0.05, **<0.01). The effect sizes of direct and indirect paths are also presented. Abbreviation: H, Shannon's diversity; $Bacteria_{All}$, all bacteria; $Bacteria_{Endo}$, endophytic bacteria; $Bacteria_{Epip}$, epiphytic bacteria; $Fungi_{All}$, all fungi; $Fungi_{Endo}$, endophytic fungi; $Fungi_{epip}$, epiphytic fungi; FT_{pc1}, the first PCA axis on the nine functional traits studied; MAT, mean annual temperature.

Figure. S7 Piecewise structural equation models (pSEMs) exploring the effects of mean annual temperature and leaf functional traits on phyllosphere bacterial and fungi richness. Standardized regression coefficients and significance are given (*<0.05, **<0.01). Abbreviation: S, richness; $Bacteria_{All}$, all bacteria; $Bacteria_{Endo}$, endophytic bacteria; $Bacteria_{Epip}$, epiphytic bacteria; $Fungi_{All}$, all fungi; $Fungi_{Endo}$, endophytic fungi; $Fungi_{epip}$, epiphytic fungi; FT_{pc1}, the first PCA axis on the nine functional traits studied; MAT, mean annual temperature.

Figure. S8 Piecewise structural equation models (pSEMs) exploring the effects of mean annual temperature and leaf functional traits on phyllosphere bacterial and fungi Shannon's diversity. Standardized regression coefficients and significance are given (*<0.05, **<0.01). Abbreviation: H, Shannon's diversity; $Bacteria_{All}$, all bacteria; $Bacteria_{Endo}$, endophytic bacteria; $Bacteria_{Epip}$, epiphytic bacteria; $Fungi_{All}$, all fungi; $Fungi_{Endo}$, endophytic fungi; $Fungi_{epip}$, epiphytic fungi; FT_{pc1}, the first PCA axis on the nine functional traits studied; MAT, mean annual temperature.

Figure. S9 Heatmap that shows relationship between plant functional traits and specific microbial

taxa (in the phyla level).

Table S1 Summary of the main characteristics of sampling sites along an elevational gradient on Changbai Mountain.

Table S2 Geographic information of the studied sites.

Table S3 Functional traits and their functions.

Table S4 Loadings of the Principal Component Analysis for trait values.

Table S5 AIC value for predicting the relationship between phyllosphere microbial richness and elevation(elevation^2). Bold represents the optimal model based on AIC. *: $P < 0.01$.

Table S6 AIC value for predicting the relationship between phyllosphere microbial Shannon index and elevation (elevation^2). Bold represents the optimal model based on AIC. *: $P < 0.01$.

Table S7 The direct, indirect, and total standardized effects of mean annual temperature and leaf functional traits on phyllosphere bacterial and fungal richness derived from the pierce structural equation models. Models are presented in Fig. 4. Only significant effects are shown.

Table S8 The direct, indirect, and total standardized effects of mean annual temperature and leaf functional traits on phyllosphere bacterial and fungal Shannon index derived from the pierce structural equation models. Models are presented in Fig. S5. Only significant effects are shown.

Fig. S1.

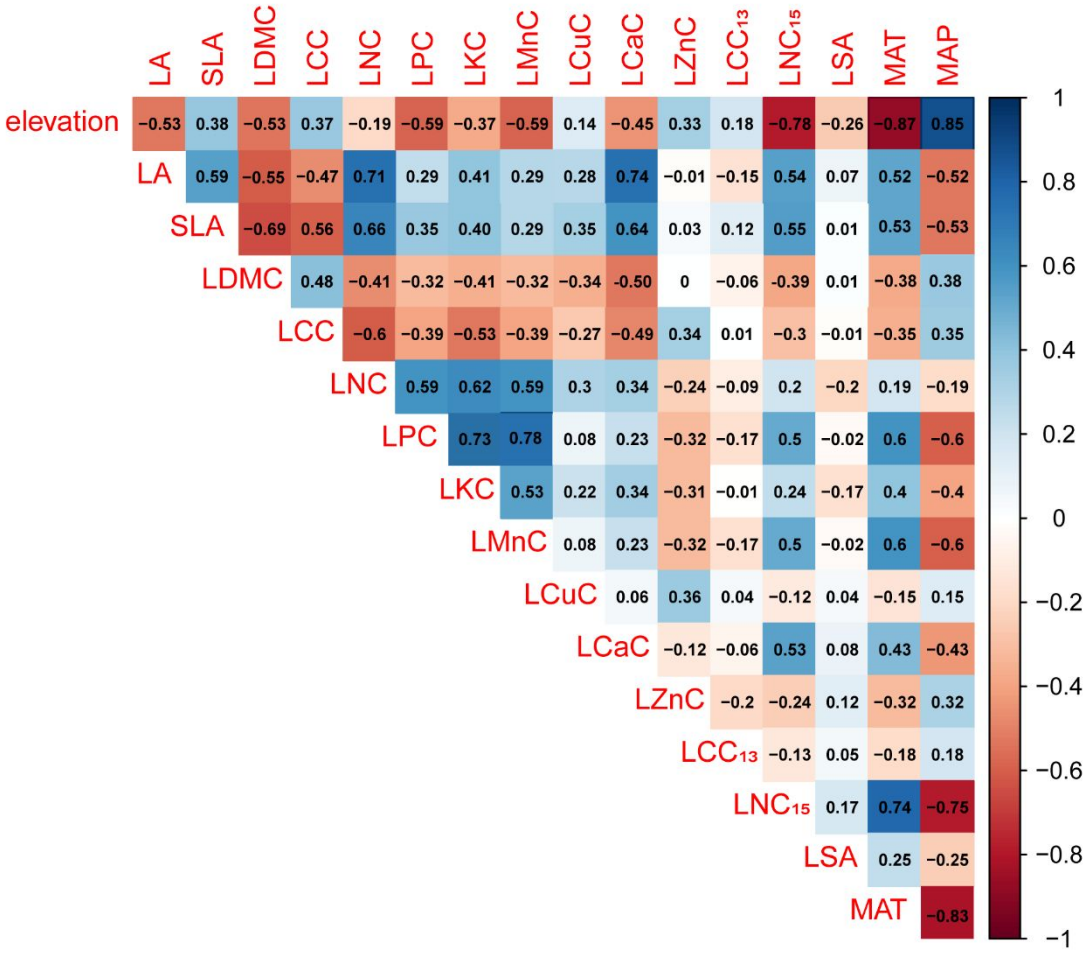
LA
SLA
LDMC
LCC
LNC
LPC
LKC
LMnC
LCuC
LCaC
LZnC
LCC13
LNC15
LSA
MAT
MAP
elevation −0.53 0.38 −0.53 0.37 −0.19 −0.59 −0.37 −0.59 0.14 −0.45 0.33 0.18 −0.78 −0.26 −0.87 0.85
LA 0.59 −0.55 −0.47 0.71 0.29 0.41 0.29 0.28 0.74 −0.01 −0.15 0.54 0.07 0.52 −0.52
SLA −0.69 0.56 0.66 0.35 0.40 0.29 0.35 0.64 0.03 0.12 0.55 0.01 0.53 −0.53
LDMC 0.48 −0.41 −0.32 −0.41 −0.32 −0.34 −0.50 0 −0.06 -0.39 0.01 −0.38 0.38
LCC −0.6 −0.39 −0.53 −0.39 −0.27 −0.49 0.34 0.01 −0.3 −0.01 −0.35 0.35
LNC 0.59 0.62 0.59 0.3 0.34 −0.24 −0.09 0.2 −0.2 0.19 −0.19
LPC 0.73 0.78 0.08 0.23 −0.32 −0.17 0.5 −0.02 0.6 −0.6
LKC 0.53 0.22 0.34 −0.31 −0.01 0.24 −0.17 0.4 −0.4
LMnC 0.08 0.23 −0.32 −0.17 0.5 −0.02 0.6 −0.6
LCuC 0.06 0.36 0.04 −0.12 0.04 −0.15 0.15
LCaC −0.12 −0.06 0.53 0.08 0.43 −0.43
LZnC −0.2 −0.24 0.12 −0.32 0.32
LCC13 −0.13 0.05 −0.18 0.18
LNC15 0.17 0.74 −0.75
LSA 0.25 −0.25
MAT −0.83
1
0.8
0.6
0.4
0.2
0
−0.2
−0.4
−0.6
−0.8
−1

Fig. S2

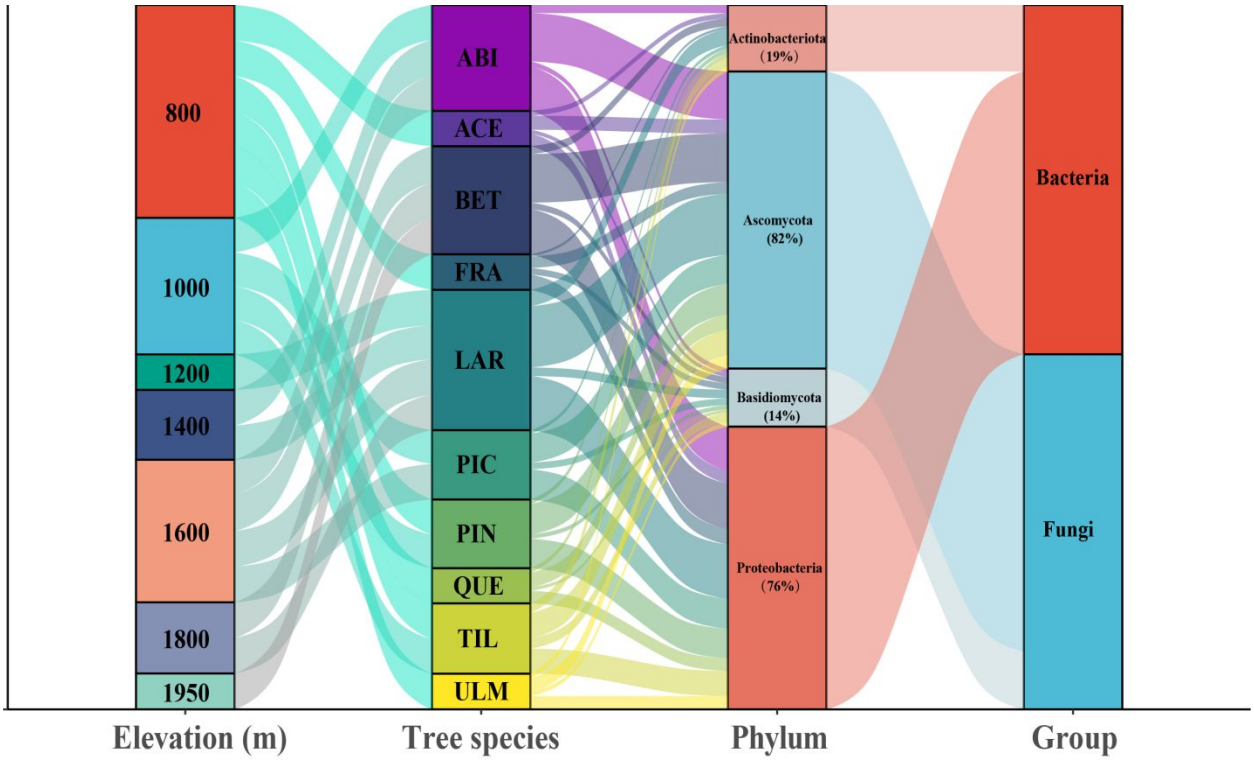

Fig. S3

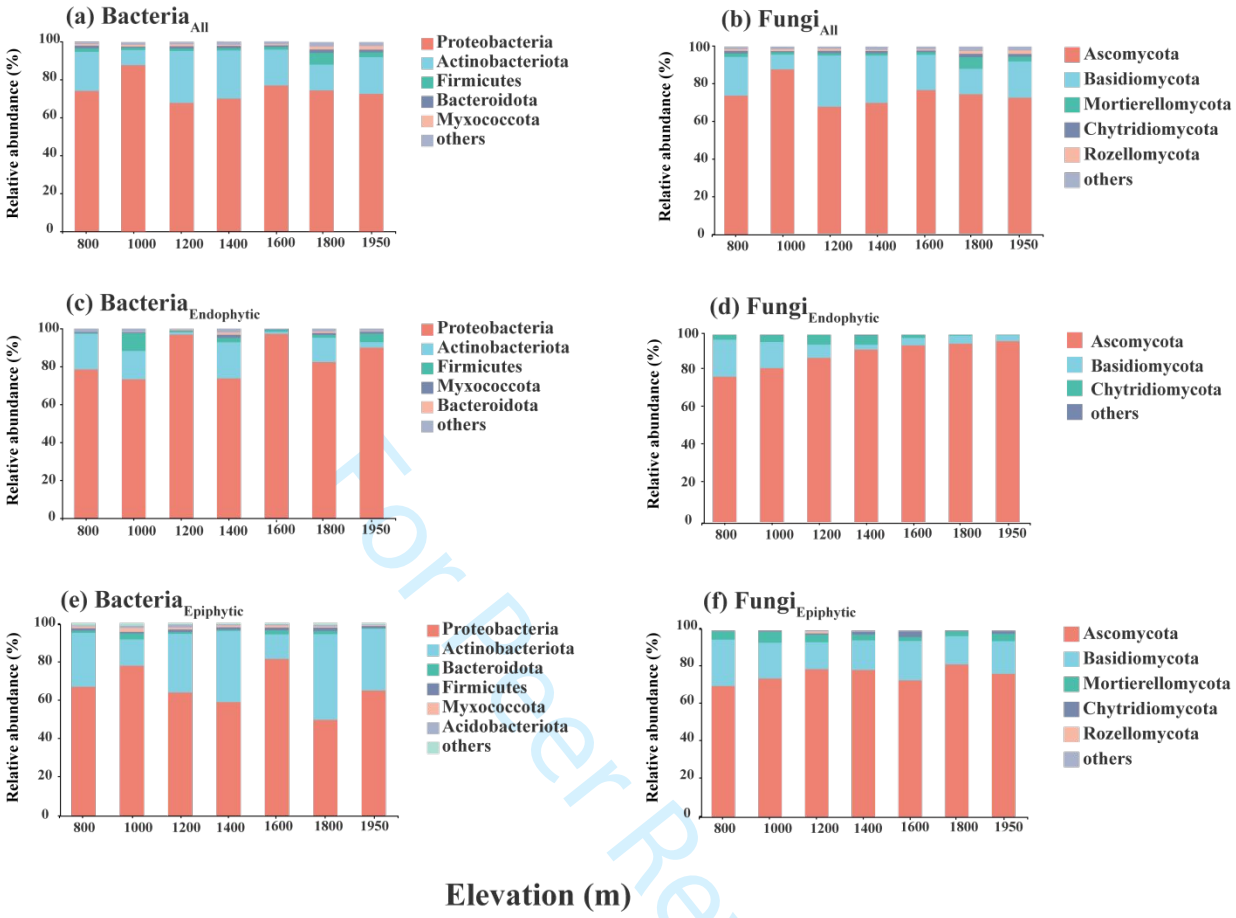

Fig. S4

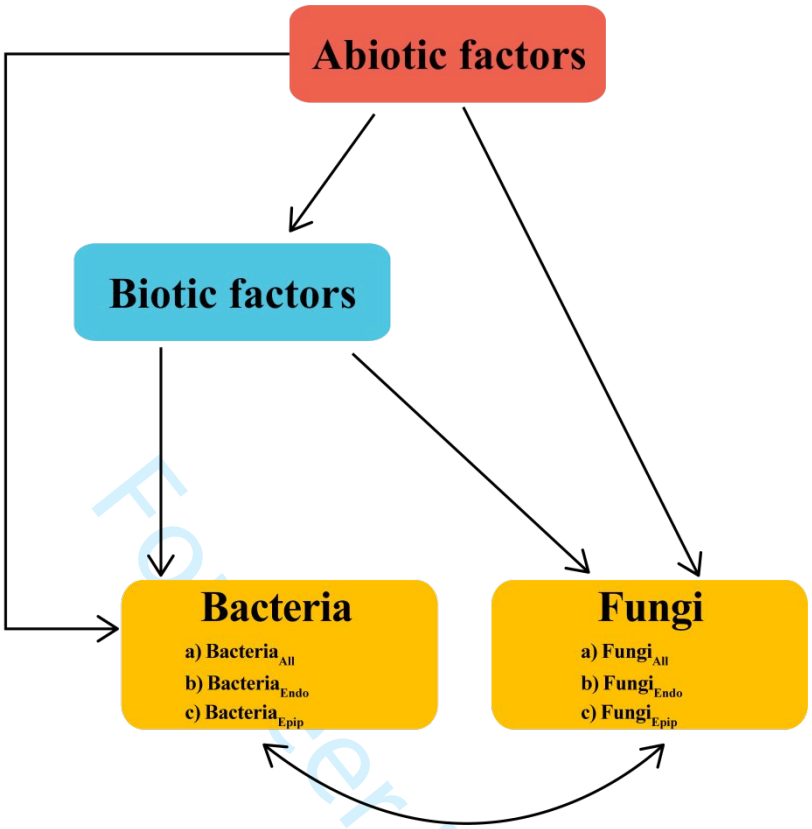

Fig. S5

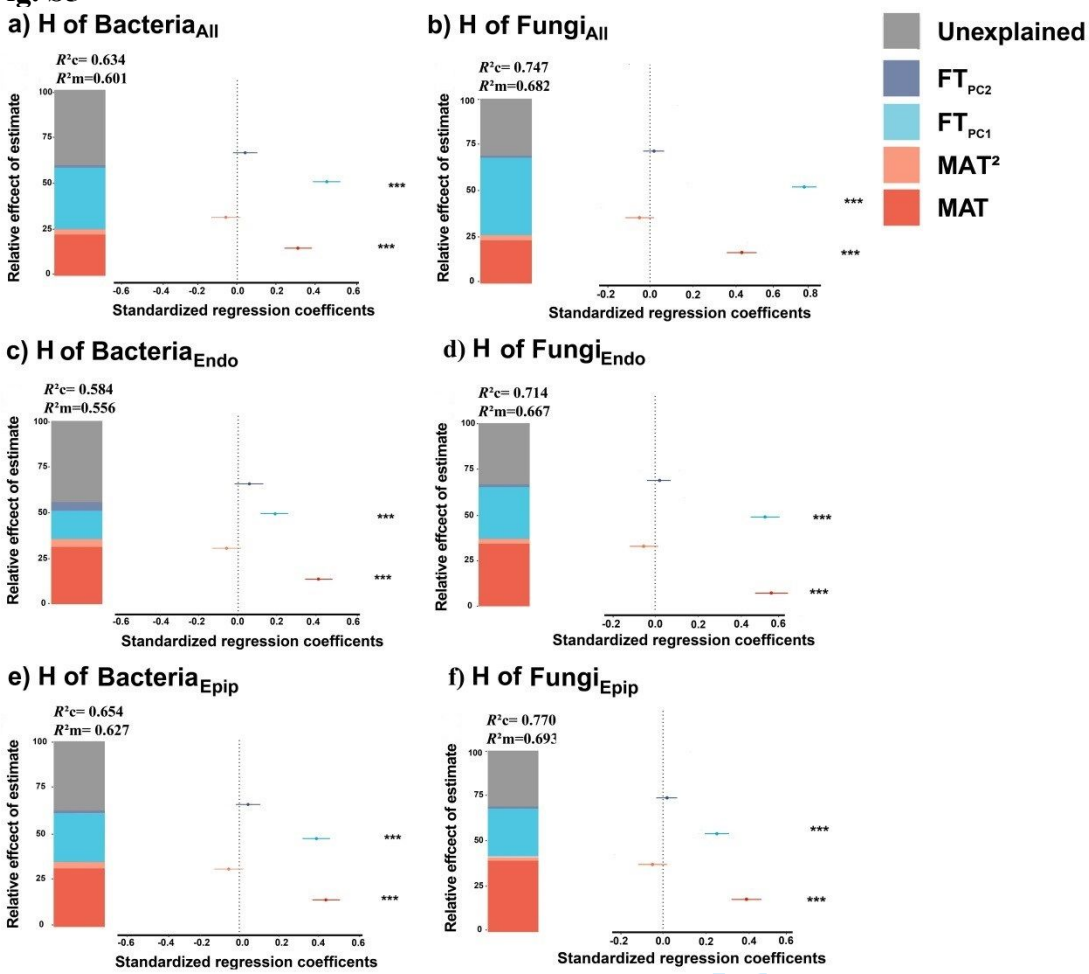
a) H of Bacteria$_{All}$
R^2c= 0.634
R^2m=0.601
b) H of Fungi$_{All}$
R^2c= 0.747
R^2m=0.682
c) H of Bacteria$_{Endo}$
R^2c= 0.584
R^2m=0.556
d) H of Fungi$_{Endo}$
R^2c= 0.714
R^2m=0.667
e) H of Bacteria$_{Epip}$
R^2c= 0.654
R^2m= 0.627
f) H of Fungi$_{Epip}$
R^2c= 0.770
R^2m=0.693
Relative effcect of estimate
Standardized regression coefficents
***
Unexplained
FT$_{PC2}$
FT$_{PC1}$
MAT²
MAT

Fig. S6

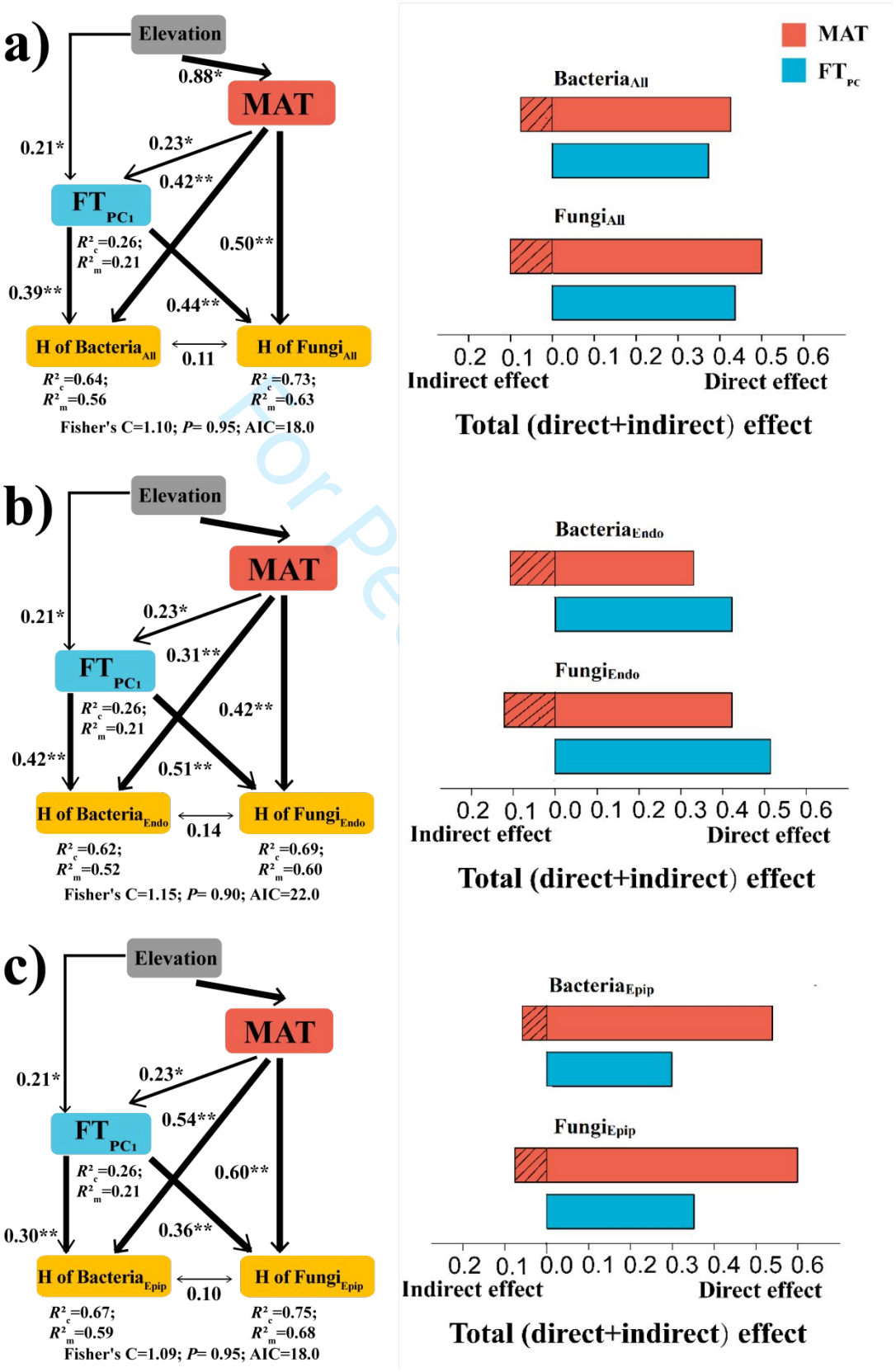
a)
Elevation
MAT
0.88*
0.21*
0.23*
0.42**
FT PC1
R²c=0.26; R²m=0.21
0.50**
0.39**
0.44**
H of Bacteria All
0.11
H of Fungi All
R²c=0.64; R²m=0.56
R²c=0.73; R²m=0.63
Fisher's C=1.10; P= 0.95; AIC=18.0
b)
Elevation
MAT
0.21*
0.23*
0.31**
FT PC1
R²c=0.26; R²m=0.21
0.42**
0.42**
0.51**
H of Bacteria Endo
0.14
H of Fungi Endo
R²c=0.62; R²m=0.52
R²c=0.69; R²m=0.60
Fisher's C=1.15; P= 0.90; AIC=22.0
c)
Elevation
MAT
0.21*
0.23*
0.54**
FT PC1
R²c=0.26; R²m=0.21
0.60**
0.30**
0.36**
H of Bacteria Epip
0.10
H of Fungi Epip
R²c=0.67; R²m=0.59
R²c=0.75; R²m=0.68
Fisher's C=1.09; P= 0.95; AIC=18.0
MAT
FT PC
Bacteria All
Fungi All
0.2 0.1 0.0 0.1 0.2 0.3 0.4 0.5 0.6
Indirect effect
Direct effect
Total (direct+indirect) effect
Bacteria Endo
Fungi Endo
0.2 0.1 0.0 0.1 0.2 0.3 0.4 0.5 0.6
Indirect effect
Direct effect
Total (direct+indirect) effect
Bacteria Epip
Fungi Epip
0.2 0.1 0.0 0.1 0.2 0.3 0.4 0.5 0.6
Indirect effect
Direct effect
Total (direct+indirect) effect

Fig. S7

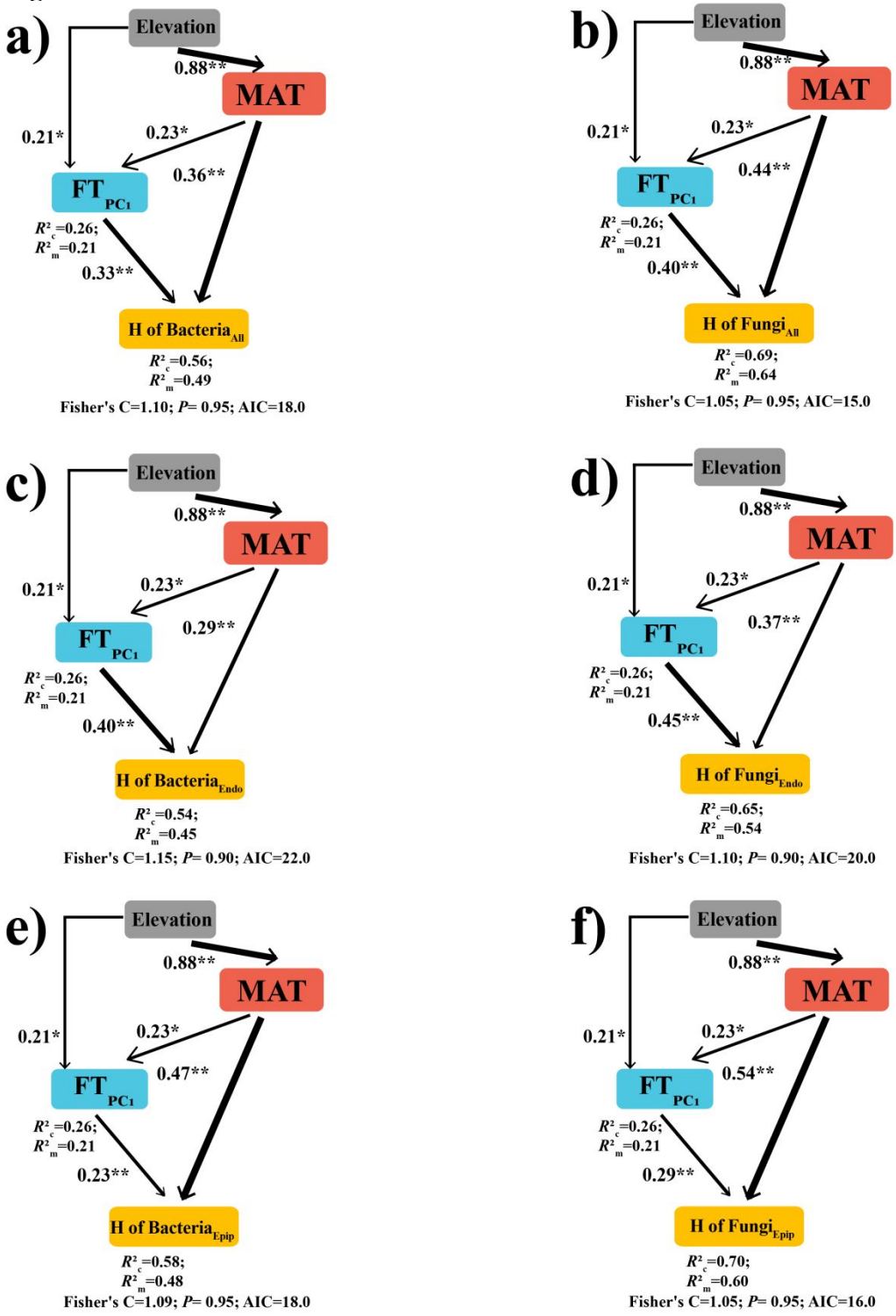
a)
Elevation
0.88**
MAT
0.21*
0.23*
0.36**
FT PC1
R²c=0.26;
R²m=0.21
0.33**
H of Bacteria All
R²c=0.56;
R²m=0.49
Fisher's C=1.10; P= 0.95; AIC=18.0
b)
Elevation
0.88**
MAT
0.21*
0.23*
0.44**
FT PC1
R²c=0.26;
R²m=0.21
0.40**
H of Fungi All
R²c=0.69;
R²m=0.64
Fisher's C=1.05; P= 0.95; AIC=15.0
c)
Elevation
0.88**
MAT
0.21*
0.23*
0.29**
FT PC1
R²c=0.26;
R²m=0.21
0.40**
H of Bacteria Endo
R²c=0.54;
R²m=0.45
Fisher's C=1.15; P= 0.90; AIC=22.0
d)
Elevation
0.88**
MAT
0.21*
0.23*
0.37**
FT PC1
R²c=0.26;
R²m=0.21
0.45**
H of Fungi Endo
R²c=0.65;
R²m=0.54
Fisher's C=1.10; P= 0.90; AIC=20.0
e)
Elevation
0.88**
MAT
0.21*
0.23*
0.47**
FT PC1
R²c=0.26;
R²m=0.21
0.23**
H of Bacteria Epip
R²c=0.58;
R²m=0.48
Fisher's C=1.09; P= 0.95; AIC=18.0
f)
Elevation
0.88**
MAT
0.21*
0.23*
0.54**
FT PC1
R²c=0.26;
R²m=0.21
0.29**
H of Fungi Epip
R²c=0.70;
R²m=0.60
Fisher's C=1.05; P= 0.95; AIC=16.0

Fig. S8

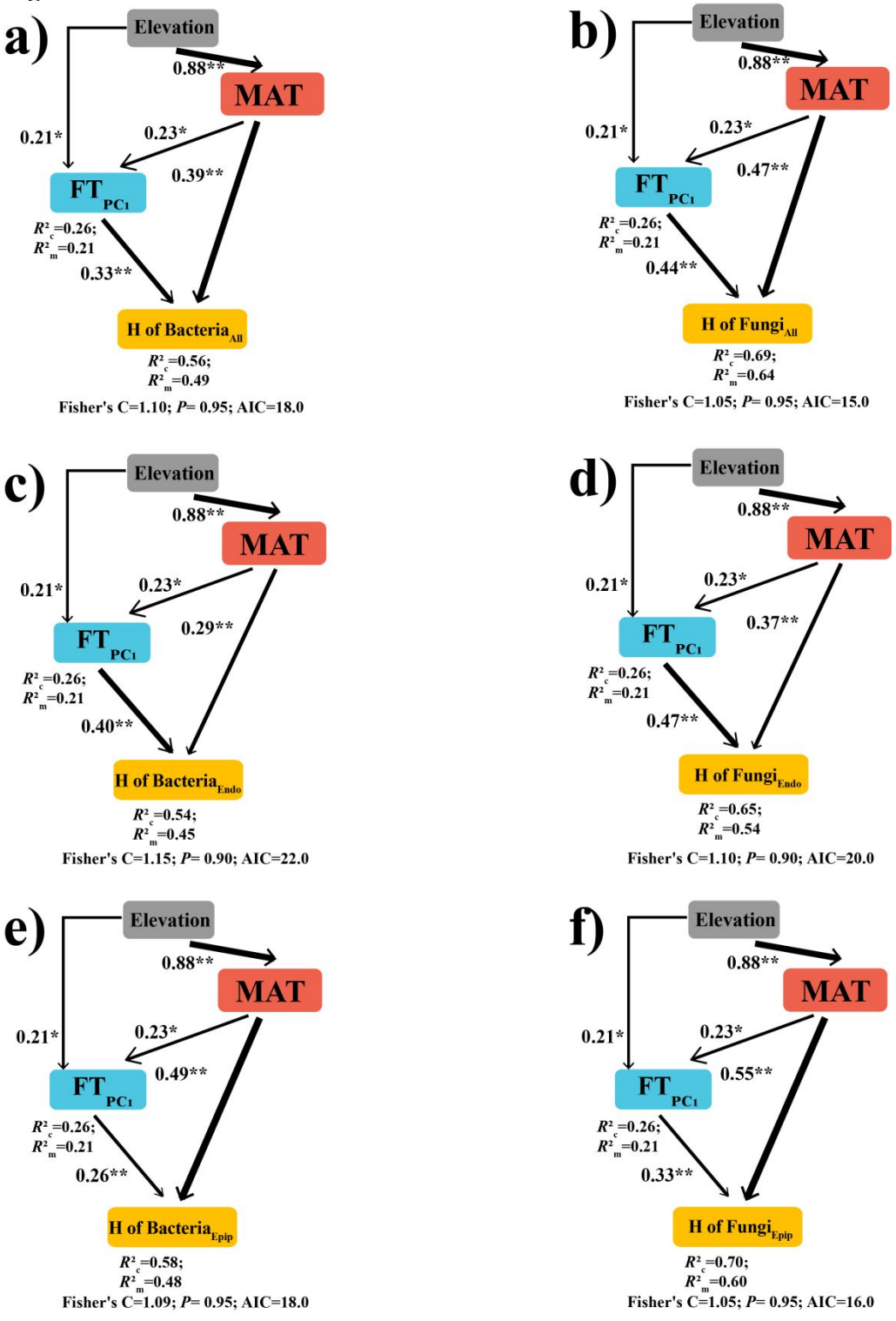
a)
Elevation
MAT
FT PC1
H of Bacteria All
0.88**
0.21*
0.23*
0.39**
0.33**
R²c=0.26; R²m=0.21
R²c=0.56; R²m=0.49
Fisher's C=1.10; P= 0.95; AIC=18.0
b)
Elevation
MAT
FT PC1
H of Fungi All
0.88**
0.21*
0.23*
0.47**
0.44**
R²c=0.26; R²m=0.21
R²c=0.69; R²m=0.64
Fisher's C=1.05; P= 0.95; AIC=15.0
c)
Elevation
MAT
FT PC1
H of Bacteria Endo
0.88**
0.21*
0.23*
0.29**
0.40**
R²c=0.26; R²m=0.21
R²c=0.54; R²m=0.45
Fisher's C=1.15; P= 0.90; AIC=22.0
d)
Elevation
MAT
FT PC1
H of Fungi Endo
0.88**
0.21*
0.23*
0.37**
0.47**
R²c=0.26; R²m=0.21
R²c=0.65; R²m=0.54
Fisher's C=1.10; P= 0.90; AIC=20.0
e)
Elevation
MAT
FT PC1
H of Bacteria Epip
0.88**
0.21*
0.23*
0.49**
0.26**
R²c=0.26; R²m=0.21
R²c=0.58; R²m=0.48
Fisher's C=1.09; P= 0.95; AIC=18.0
f)
Elevation
MAT
FT PC1
H of Fungi Epip
0.88**
0.21*
0.23*
0.55**
0.33**
R²c=0.26; R²m=0.21
R²c=0.70; R²m=0.60
Fisher's C=1.05; P= 0.95; AIC=16.0

Fig. S9

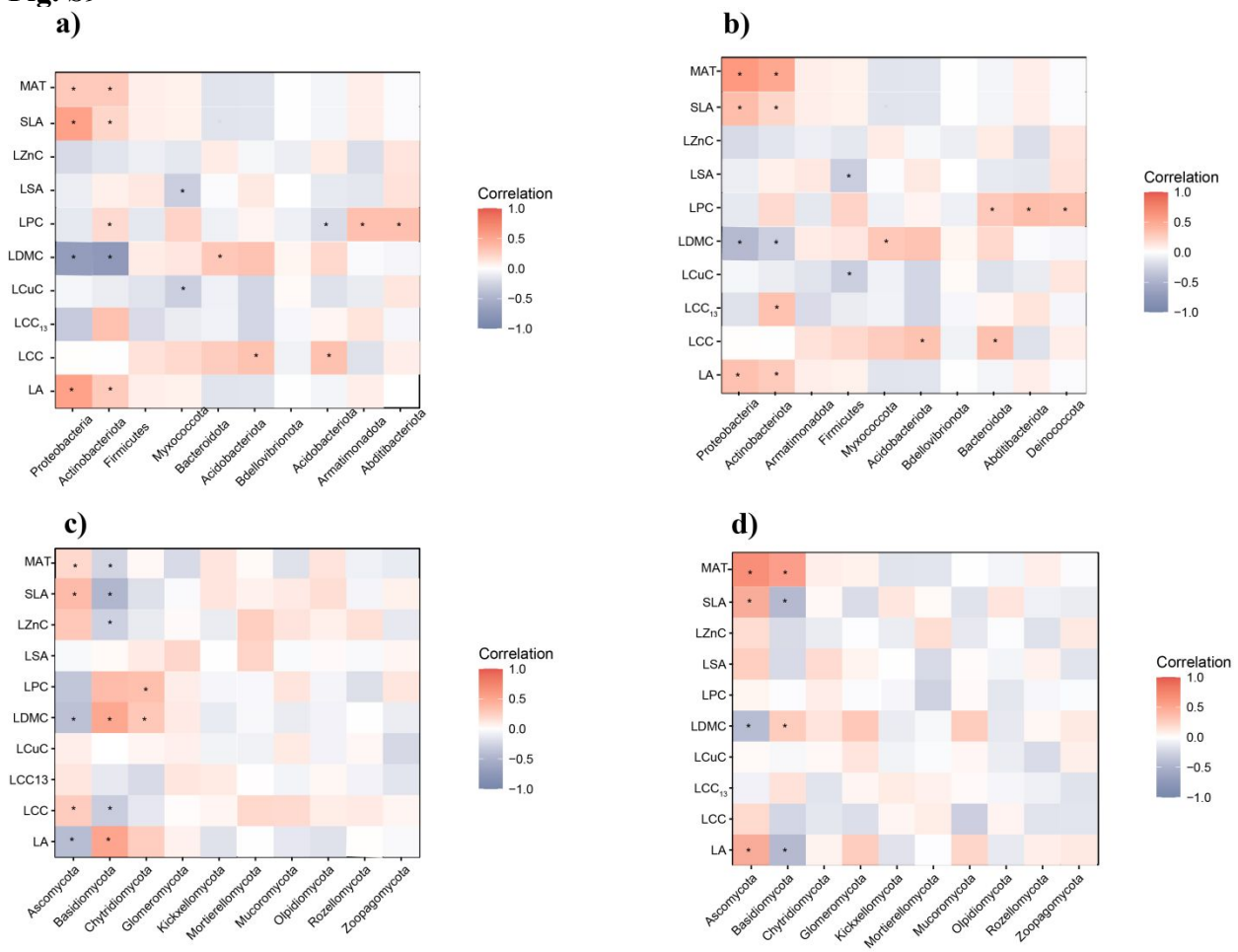
a)
MAT
SLA
LZnC
LSA
LPC
LDMC
LCuC
LCC13
LCC
LA
Proteobacteria
Actinobacteriota
Firmicutes
Myxococcota
Bacteroidota
Acidobacteriota
Bdellovibrionota
Acidobacteriota
Armatimonadota
Abditibacteriota
Correlation
1.0
0.5
0.0
−0.5
−1.0
b)
MAT
SLA
LZnC
LSA
LPC
LDMC
LCuC
LCC13
LCC
LA
Proteobacteria
Actinobacteriota
Armatimonadota
Firmicutes
Myxococcota
Acidobacteriota
Bdellovibrionota
Bacteroidota
Abditibacteriota
Deinococcota
Correlation
1.0
0.5
0.0
−0.5
−1.0
c)
MAT
SLA
LZnC
LSA
LPC
LDMC
LCuC
LCC13
LCC
LA
Ascomycota
Basidiomycota
Chytridiomycota
Glomeromycota
Kickxellomycota
Mortierellomycota
Mucoromycota
Olpidiomycota
Rozellomycota
Zoopagomycota
Correlation
1.0
0.5
0.0
−0.5
−1.0
d)
MAT
SLA
LZnC
LSA
LPC
LDMC
LCuC
LCC13
LCC
LA
Ascomycota
Basidiomycota
Chytridiomycota
Glomeromycota
Kickxellomycota
Mortierellomycota
Mucoromycota
Olpidiomycota
Rozellomycota
Zoopagomycota
Correlation
1.0
0.5
0.0
−0.5
−1.0

Table S1

Elevation	Vegetation type	Tree species name	Abbreviation
800m	*Mixed coniferous–broadleaf forest*	*Ulmus_japonica*	*ULM*
		Quercus_mongolica	*QUE*
		Acer_mono	*ACE*
		Tilia_amurensis	*TIL*
		Pinus_koraiensis	PIN
		Fraxinus_mandshurica	*FRA*
1000m	*Mixed coniferous–broadleaf forest*	*Pinus_koraiensis*	*PIN*
		Tilia_amurensis	*TIL*
		Abies_nephrolepis	*ABI*
		Picea_jezoensis	*PIC*
1200m	*Coniferous forest*	*Larix_gmelinii*	*LAR*
1400m	*Coniferous forest*	*Abies_nephrolepis*	ABI
		Larix_gmelinii	LAR
1600m	*Coniferous* forest	*Betula_ermanii*	BET
		Abies_nephrolepis	ABI
		Larix_gmelinii	LAR
		Picea_jezoensis	PIC
1800m	Birch forest	*Larix_gmelinii*	LAR
		Betula_ermanii	BET
1950m	Birch forest	*Betula_ermanii*	BET

Table S2

Plot	Latitude	Longitude	Elevation
1	42.2124041	128.4214579	800
2	42.2111062	128.4297998	800
3	42.35094433	127.9687601	800
4	42.3509615	127.9657993	800
5	42.3515333	127.961157	800
6	42.23425683	128.1452635	1000
7	42.23435033	128.1487417	1000
8	42.2399925	128.139942	1000
9	42.235203	128.155823	1000
10	42.23456183	128.151056	1000
11	42.16324833	128.1575617	1200
12	42.1641135	128.1527838	1200
13	42.16171583	128.1496682	1200
14	42.16287717	128.1505947	1200
15	42.16145717	128.1504003	1200
16	42.1111685	128.1021245	1400
17	42.11104967	128.1034917	1400
18	42.11009183	128.1035272	1400
19	42.11084033	128.1009102	1400
20	42.11062467	128.1025682	1400
21	42.0883485	128.0724015	1600
22	42.08745117	128.0736145	1600
23	42.08791617	128.0714043	1600
24	42.08721617	128.0710297	1600
25	42.08674417	128.0724183	1600
26	42.0671645	128.0676052	1800
27	42.06625783	128.0674132	1800
28	42.06493917	128.0665682	1800
29	42.06547567	128.0670377	1800
30	42.06414983	128.067009	1800
31	42.06086367	128.0684068	1950
32	42.06011817	128.0182908	1950
33	42.0597485	128.0676098	1950
34	42.05933067	128.0679163	1950
35	42.058869	128.0683998	1950

Table S3

Abbreviations	Functional traits	Functions
LA	Leaf Area	Resource allocation capacity
SLA	Specific Leaf Area	Resource allocation capacity
LDMC	Leaf Dry Matter Content	Resource allocation capacity
LCC_{13}	Leaf Stable Carbon 13 Content	Water utilization efficiency
LNC_{15}	Leaf Stable Nitrogen 15 Content	Resource utilization efficiency
LCC	Leaf Carbon Content	Plant photosynthesis
LNC	Leaf Nitrogen Content	Plant photosynthesis
LPC	Leaf Phosphorus Content	Plant photosynthesis
LKC	Leaf Potassium Content	Plant photosynthesis
LCaC	Leaf Calcium Content	Plant metabolism
LMnC	Leaf Manganese Content	Plant metabolism
LCuC	Leaf Copper Content	Plant metabolism; resistance to diseases, pests and microbes
LZnC	Leaf Zinc Content	Plant metabolism; resistance to diseases, pests and microbes
LSA	Leaf Stomatal Area	Transpiration, photosynthesis

Table S4

Traits	PC1 (46.9%)	PC2 (28.7 %)
LA	**0.45**	
SLA	**0.51**	-0.28
LDMC	**-0.40**	
LCC	-0.40	
LPC	-0.39	-0.33
LCuC		**0.592**
LZnC		**0.649**
LCC_{13}		
LSA		

Table S5

	Predictors	AIC	Likelihood ratio test (Elevation vs. Elevation^2)
All bacterial richness	Elevation	**234.673**	< 0.001
	Elevation^2	274.379	
Endophytic bacterial richness	Elevation	**224.673**	< 0.001
	Elevation^2	254.142	
Epiphytic bacterial richness	Elevation	**227.824**	< 0.001
	Elevation^2	265.015	
All fungal richness	Elevation	**183.221**	< 0.001
	Elevation^2	202.594	
Endophytic fungal richness	Elevation	**179.002**	< 0.001
	Elevation^2	194.556	
Epiphytic fungal richness	Elevation	**184.017**	< 0.001
	Elevation^2	199.754	

Table S6

	Predictors	**AIC**	**Likelihood ratio test (Elevation vs. Elevation^2)**
All bacterial Shannon index	Elevation	**227.606**	< 0.001
	Elevation^2	256.386	
Endophytic bacterial Shannon index	Elevation	**211.750**	< 0.001
	Elevation^2	242.786	
Epiphytic bacterial Shannon index	Elevation	**220.554**	< 0.001
	Elevation^2	246.012	
All fungal Shannon index	Elevation	**179.665**	< 0.001
	Elevation^2	203.457	
Endophytic fungal Shannon index	Elevation	**169.014**	< 0.001
	Elevation^2	187.581	
Epiphytic fungal Shannon index	Elevation	**180.171**	< 0.001
	Elevation^2	188.600	

Table S7

	MAT (Total)	MAT (Direct)	MAT (Indirect)	FT_{PC1}
All bacteria	0.476	0.395	0.081	0.358
Endophytic baceria	0.399	0.305	0.094	0.417
Epiphytic baceria	0.582	0.524	0.058	0.258
All fungi	0.567	0.474	0.093	0.412
Endophytic fungi	0.498	0.388	0.110	0.491
Epiphytic fungi	0.647	0.572	0.075	0.333

Table S8 The direct, indirect, and total standardized effects of mean annual temperature and leaf functional traits on phyllosphere bacterial and fungal Shannon index derived from the pierce structural equation models. Models are presented in Fig. 5. Only significant effects are showed.

	MAT (Total)	**MAT (Direct)**	**MAT (Indirect)**	**FT_{PC1}**
All bacteria	0.508	0.421	0.087	0.386
Endophytic baceria	0.403	0.308	0.095	0.423
Epiphytic baceria	0.603	0.535	0.068	0.304
All fungi	0.629	0.531	0.098	0.436
Endophytic fungi	0.538	0.424	0.114	0.508
Epiphytic fungi	0.684	0.603	0.081	0.359